AFRL-VS-TR-2003-1530
E.R.P., No. 1251

SSI-TR-399

# User's Manual for SAG-2, SHARC/SAMM Atmosphere Generator

**Robert M. Shroll, Steven Adler-Golden, and James W. Duff**

Spectral Sciences, Inc.
99 South Bedford Street, Suite 7
Burlington, MA 01803-5169

**James H. Brown**

Air Force Research Laboratory
29 Randolph Road
Hanscom AFB, MA 01731-3010

14 October 2003



**AIR FORCE RESEARCH LABORATORY**
**Space Vehicles Directorate**
**29 Randolph Rd**
**AIR FORCE MATERIEL COMMAND**
**Hanscom AFB, MA 01731-3010**

This technical report has been reviewed and is approved for publication.

/ signed /
John B. Wissler, LtCol, USAF, Director
Battlespace Environment Division

/ signed /
James B. Brown
Author

/ signed /
Robert R. Beland, Chief
Space Weather Center of Excellence

This report has been reviewed by the Public Affairs Office (PA) and is releasable to the National Technical Information Service (NTIS).

Qualified requestors may obtain additional copies form the Defense Technical Information Center (DTIC). All others should apply to the National Technical Information Service.

If your address has changed, if you wish to be removed from the mailing list, or if the addressee is no longer employed by your organization, please notify AFRL/VSIM, 29 Randolph Rd., Hanscom AFB, MA 01731-3010. This will assist us in maintaining a current mailing list.

Do not return copies of this report unless contractual obligations or notices on a specific document require that it be returned.

# REPORT DOCUMENTATION PAGE

*Form Approved*
*OMB No. 0704-0188*



| 1. REPORT DATE *(DD-MM-YYYY)* | 2. REPORT TYPE | 3. DATES COVERED *(From - To)* |
|---|---|---|
| 14-10-2003 | Scientific, Interim | |

**4. TITLE AND SUBTITLE**
User's Manual for SAG-2, SHARC/SAMM Atmosphere Generator

**5a. CONTRACT NUMBER**
F19628-98-C-0050

**5b. GRANT NUMBER**

**5c. PROGRAM ELEMENT NUMBER**
63880C

**6. AUTHOR(S)**
Robert Shroll*, Steven Adler-Golden*, James W. Duff*, James H. Brown

**5d. PROJECT NUMBER**
6403, 3352

**5e. TASK NUMBER**
6403BD, 3352BD

**5f. WORK UNIT NUMBER**
6403BDAA, 3352BDA1

**7. PERFORMING ORGANIZATION NAME(S) AND ADDRESS(ES)**
Air Force Research Laboratory/VSBYB
29 Randolph Road
Hanscom AFB, MA 01731-3010

**8. PERFORMING ORGANIZATION REPORT NUMBER**
SSI-TR-399
AFRL-VS-TR-2003-1530
Environmental Research Papers, No. 1251

**9. SPONSORING/MONITORING AGENCY NAME(S) AND ADDRESS(ES)**

**10. SPONSOR/MONITOR'S ACRONYM(S)**

**11. SPONSOR/MONITOR'S REPORT NUMBER(S)**

**12. DISTRIBUTION/AVAILABILITY STATEMENT**
Approved for Public Release; Distribution Unlimited

**13. SUPPLEMENTARY NOTES**
* Spectral Sciences, Inc., 99 South Bedford St., Suite 7, Burlington, MA 01803-5169. Both Spectral Sciences and AFRL scientists participated in this work; both SSI and AFRL are considered performing organizations.

**14. ABSTRACT**
The SHARC Atmosphere Generator (SAG) is a stand-alone, interactive program that utilizes a combination of empirical models to generate atmospheric profiles for Air Force IR radiation codes that account for systematic variability of the atmosphere, including solar terminator effects. Using information on the day of the year, local time, solar and geomagnetic activity indices, etc., SAG reasonably models the variabilities in temperature and $CO_2$, $O_3$, OH, NO, $H_2O$ and O densities. For other species, diurnally-averaged profiles are derived from recent climatology databases or other standard tabulations. The SAG output files support SHARC, SAMM, and MODTRAN.

**15. SUBJECT TERMS**
Atmosphere Infrared Variability Profile
SHARC SAMM MODTRAN MSIS

| 16. SECURITY CLASSIFICATION OF: | | | 17. LIMITATION OF ABSTRACT | 18. NUMBER OF PAGES | 19a. NAME OF RESPONSIBLE PERSON |
|---|---|---|---|---|---|
| a. REPORT | b. ABSTRACT | c. THIS PAGE | | | James H. Brown |
| UNCL | UNCL | UNCL | UNL | | 19b. TELEPHONE NUMBER *(Include area code)* 781 377-4412 |

## TABLE OF CONTENTS

## LIST OF ILLUSTRATIONS

## LIST OF ILLUSTRATIONS (Continued)



## LIST OF TABLES

## Preface

This report serves two purposes. First, it serves as the Users' Manual for the SHARC/SAMM Atmosphere Generator, a stand-alone program that generates atmospheric profiles for Air Force IR radiation codes that account for systematic variability of the atmosphere. For this reason it includes the results of work done by scientists at Spectral Sciences, Inc., who incorporated the SNOE database for NO density, URAP $H_2O$ database, revised O atom profiles, and revised H atom profiles, in addition to documenting the work of Air Force Research Laboratory scientists, who incorporated the NRLMSISE-00 database, incorporated choices for Geodetic or Geocentric Latitude input, and tested and verified the code. Second, this report also serves as the final scientific report for in-house work unit 3352BDA1.

The authors thank R. Kennett (Spectral Sciences Inc.) for numerous improvements to the code, G.P. Anderson (AFRL) for providing the NRL Trace Climatology database, R. Rodrigo (Instituto de Astrofisica de Andalucia) for providing theoretical profiles, and R. Sharma for valuable discussions. The work done by Spectral Sciences, Inc. was funded under Air Force contract F19628-93-C-0050.

# 1. INTRODUCTION

The Air Force Strategic High-Altitude Radiance Code (SHARC) and the SAMM (SHARC And MODTRAN Merged) code have been developed to address the strategic requirements for modeling infrared (IR) background radiation and structure in the upper atmosphere. One of their most critical applications is in modeling radiance variations, which can occur over a wide range of spatial and temporal scales. Short-term and small-scale variations associated with random processes can be characterized and predicted statistically. On the other hand, systematic variations, which can be predicted deterministically, may be quite large and thus play an important role in setting the overall background radiance level for a given bandpass. In particular, at the solar terminator, large radiance variations can occur over a small (several-degree) range of solar zenith angle due to photochemical processes in the atmosphere.

The SHARC Atmosphere Generator (SAG) has been designed to allow the major known, systematic variabilities in the atmosphere, including terminator and other diurnal effects, to be practically incorporated in strategic IR radiance calculations. SAG is presently implemented as a FORTRAN subroutine, which may be run via the supplied or user furnished driver program. This allows SAG to be run interactively or in a batch processing mode by looping over atmospheric dependencies in the driver program. SAG may be used to generate an atmosphere file for use with MODTRAN and a file of species and kinetic temperature profiles compatible with SHARC and SAMM. The profiles are customized for the geophysical and geographic information input by the user.

Using information on the day of the year, local time, solar activity indices, etc., SAG reasonably models the systematic variabilities in $CO_2$, $O_3$, OH, NO, $H_2O$, and O atom densities. For other species, diurnally-averaged profiles are taken from recent databases. To facilitate use without detailed inputs, defaults are provided so that simple designators, such as day/night, season, and latitude region (low, mid, or high), can be specified as desired.

SAG draws on several existing empirical atmosphere models. Either MSISE-90[1] or NRLMSISE-00[2] may be used for the temperature and major species profiles. They provide profiles for species including $N_2$, $O_2$, O, and H as a function of altitude, latitude, longitude, universal time (UT), local solar time (LST), daily average Ap index, and the F10.7 (previous day) and F10.7A (81 day centered average) solar flux indices. The second atmosphere model is

the NRL climatology database[3] for altitudes up to 120 km. This database is used for the SHARC and SAMM species $CH_4$ and CO, and for lower portions of the $O_3$ and O profiles, as well as for the additional species $N_2O$, $NO_2$, and $HNO_3$ used in SAMM. The NRL database[3] contains mean monthly mixing ratios at 1 to 5 km altitude increments and 10° latitude increments. SAG interpolates between these values and converts to number densities using the MSISE-90 or NRLMSISE-00 total densities.

New water vapor climatology has been introduced into SAG 2.0. The new climatology was developed by the UARS Reference Atmosphere Project (URAP), whose aim is to provide a comprehensive reference description of the stratosphere based on the data recorded by instruments on the NASA Upper Atmosphere Research Satellite (UARS).[4] The URAP water vapor climatology was constructed from the HALOE (HALogen Occulation Experiment)[5], MLS (Microwave Limb Sounder Experiment),[6] and SAGE II (Stratospheric Aerosol and Gas Experiment)[7] data and presented as monthly zonal means, where the zones are designated by latitude and pressure.[8] The new climatology is a substantial improvement on CIRA-1996[9], which is based on pre-URAP data.

The Student Nitric Oxide Explorer (SNOE) database has been introduced to provide nitric oxide profiles between 97 km and 150 km.[10] The database consists of measurements of nitric oxide density in the thermosphere for the period March 11, 1998 to September 30, 2000. The data covers the latitude range of 80° S to 80° N at 5° intervals and the longitude range 180° W to 180° E at 24° intervals.

The remaining species profiles, including those for $CO_2$, OH, $SO_2$, and $NH_3$ are derived from a combination of standard concentrations[11] used in MODTRAN, photochemical or empirical models based on inputs or outputs ($CO_2$), or some combination of these (OH), as described in this report.

The following sections provide a detailed description of the SHARC/SAMM Atmosphere Generator, including operating instructions, computation methods, and examples. Appendix A summarizes the changes between SAG 0.92 and SAG 2.0, Appendix B summarizes the program structure, and Appendix C presents sample inputs and outputs.

## 2. USAGE

### 2.1 Entering Parameters

Parameters required for the calculations are passed to SAG via a driver program. In the interactive mode, parameters may be entered by the user during an interactive session with SAG. A sample session is illustrated in Appendix C. When the SAG driver is run, it first retrieves the parameters from the previous session, which are stored in the input file "drivstor.dat". When the main menu appears (see C.1 Sample Interactive Session), the user responds by typing an integer. Two of the responses ("3" and "4") lead to sub-menus. Typing "0" or "0,0" from a sub-menu returns the user to the main menu. New to SAG 2.0, in the Main Menu, is the option "6 Run QA Tests". This option will cause SAG to generate 150 different atmospheres and then run a comparison between these results and 150 previously calculated atmospheres in the file QADAT/ATM_QA.DAT. The QA Test option may be used to test the integrity of a SAG installation. When the QA test is performed the "drivstor.dat" file is overwritten.

Table 1: Parameter Menu

```
PARAMETER MENU
Current parameters are
 1    Daily Ap =  18.0
 2    F10.7 =  120.0
 3    F10.7A (81 day centered average of F10.7) =  120.0
 4    Latitude Type =  1  Latitude (- =S) =  16.6
      Latitude Type: Geocentric(0), Geodetic(1)
 5    Longitude =  25.0
 6    UT (sec) = 43200.
 7    Solar Time (hrs) =  13.67
 8    Month =  5
 9    Day =  12
 10   Year = 2002
 11   Day Number =  132
 12   Solar Zenith =  24.76
 13   H, O, URAP, SNOE, NRLMSISE-00 =  T T T T F
Enter item number [n] or [0] to return to main menu:
```

The sub-menus are used to display the current parameters and to enter new ones. The Parameter Menu lists the current values and permits the user to directly enter new values. An example Parameter Menu is shown in Table 1. The menu contains information on the day of the

year, universal time or local solar time, latitude, longitude, F10.7 daily solar flux for previous day and F10.7A 81 day centered average solar flux, and daily average Ap. The SAG version 2.0 parameter menu also contains new options for using the NRLMSISE-00 empirical model in place of MSISE-90, including the URAP or SNOE databases, and adding corrections to the O atom and H atom profiles. The latitude may be entered in either geocentric or geodetic coordinates. SAG uses geodetic coordinates in its calculations.

Table 2: Default Parameter Values

| PARAMETER | UNITS | DESIGNATOR | VALUE |
|---|---|---|---|
| Local Solar Time | Hours | Day | 12[a] |
| | | Night | 0[a] |
| Day of Year | | Winter | 66 |
| | | Spring | 157 |
| | | Summer | 248 |
| | | Fall | 339 |
| Latitude | Degrees N | Equatorial | 5 |
| | | Mid | 35 |
| | | High | 65 |
| Solar Flux | F10.7, F10.7A | Low | 70 |
| | | Medium | 120 |
| | | High | 200 |
| Geomagnetic Activity | Ap | Low | 3 |
| | | Medium | 15 |
| | | High | 75 |

[a]Longitude also set to 0°.

The Default Menu is used for entering default parameters, which are convenient for generic calculations, and for specifying a custom list of altitudes (see Subsection 2.3). The default values are given in Table 2. For example, the geocentric latitude is set to 35° when the latitude default designator "m" (mid-latitude) is entered. The letter "m" will then appear at the end of the "latitude" line in the menu listing. The absence of a designator letter indicates that a directly-entered parameter is in use.

One can re-enter any parameter or either sub-menu any number of times. By using both sub-menus, any combination of default parameters and directly entered parameters can be chosen. To save a particular set of parameter values for future re-use, one can save a copy of "drivstor.dat" under a different file name. This file can then be recopied to "drivstor.dat" when the SAG rerun is needed.

### 2.2 Parameter Relationships and Permitted Values

As there are more parameters in SAG than there are independent variables, some parameters are constrained. For example, Universal Time (UT) and Local Solar Time (LST) are mutually dependent for a given longitude. When either UT or LST are entered, the program automatically updates the other parameter. When longitude is entered, LST is updated using the existing value of UT. The longitude range is −180° to 360° to allow the user to follow either the 0 to 360° or −180 to 180° convention, where 0° to 180° is defined to be West longitude. The parameter values are also checked for physical reasonableness.

Except when directly entered, the solar zenith angle (SZA) is treated as a dependent variable, being a function of the longitude, latitude, Julian day, and either LST or UT. The program automatically calculates and updates SZA when any of those parameters are entered. The SZA computed by SAG is not transferred directly to SHARC or SAMM at present. When the SZA is directly entered, the other parameters are retained except for longitude, which is recomputed.

### 2.3 Altitude and Species Lists

The list of desired altitudes and the choice of SHARC or SAMM/MODTRAN species are specified in the Default Menu. Default lists exist for SAMM, SHARC, and MODTRAN. Alternatively, a custom altitude list can be input by the user from file "drivht.dat". Line 1 contains an integer argument, 0 for outputting SHARC species only or, 1 for outputting all

SAMM/MODTRAN species (see Appendix B.5). The number of altitudes appears on line 2. Up to 200 altitudes from 0 to 300 km are allowed. The altitude list starts on line 3; the FORTRAN general input format is used, so that either integer or floating point numbers may be entered. Note that the listing in the output atmosphere file is rounded to two decimal places.

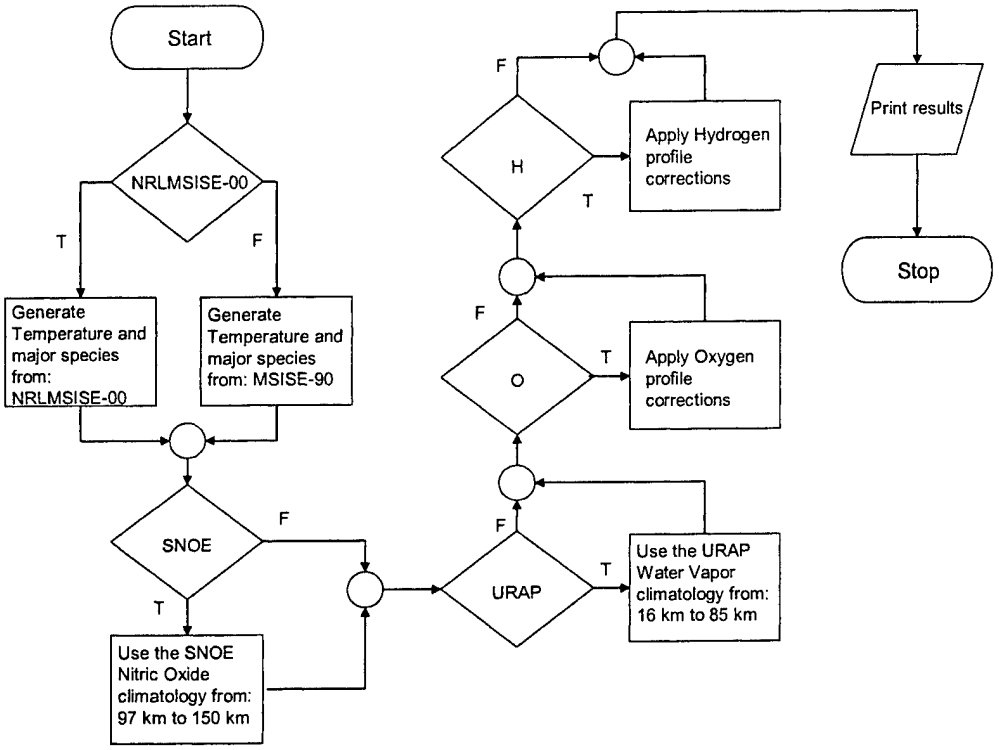


Figure 1: A flowchart explaining the new SAG 2.0 capabilities accessible through option 13 of the PARAMETER MENU. Choosing F (false) for all options returns the SAG 0.92 atmosphere.

## 2.4 SAG 2.0 Options

SAG 2.0 has several new capabilities accessed through option 13 of the PARAMETER MENU. Figure 1 shows a flowchart, which describes many of the new feature of SAG and their relation to each other. The NRLMSISE-00 option is used to choose between the two MSISE databases, which provide temperature and major species profiles. These databases along with the NRL database[3] are used by SAG to generate the minor species profiles, as described later in this manual. The SNOE and URAP database profiles for NO and $H_2O$ may be used over their

defined altitude ranges to replace the SAG 0.92 style profiles. Correction to the O and H density profile may also be included, the details of which will be presented later in the manual.

## 3. PROFILE COMPUTATIONS

This section describes how the atmospheric profiles are generated. The Temperature, $N_2$ and $O_2$ profiles are taken directly from MSISE-90 or NRLMSISE-00 and have been discussed in detail in Hedin's[1,2] papers. Brief discussions are given in the following subsections on the profiles for temperature and the remaining species.

Diurnal variations in the $CO_2$, NO, $O_3$, O, and OH densities are handled in an empirical, analytical manner in SAG using an interpolation weighting factor, W, in combination with limiting daytime and nighttime profiles:

$$X = WX_d + (1\text{-}W)X_n \tag{1}$$

Here X is the density of species, $X_d$ is the daytime (photochemical equilibrium) density and $X_n$ is the nighttime (photochemical equilibrium) density (see subsequent sections for detailed descriptions for individual species). The daytime and nighttime densities are functions of the geophysical and geographic parameters (excluding time) and the dependencies of W are discussed below.

For $O_3$, O, and OH, the chemical time constants are often comparable to or shorter than the sunrise or sunset duration. The weighting factor for these species is given by,

$$W(\theta_s) = \begin{cases} 1 & \text{if } \theta_s < \theta_{\min} \\ \dfrac{\theta_{\max} - \theta_s}{\theta_{\max} - \theta_{\min}} & \text{if } \theta_{\min} \le \theta_s \le \theta_{\max} \\ 0 & \text{if } \theta_s > \theta_{\max} \end{cases} \tag{2}$$

where $\theta_s$ is the solar zenith angle calculated 4.5 minutes prior to the current time in order to approximate the photochemical lag time. $\theta_{\min}$ and $\theta_{\max}$ are the minimum and maximum solar zenith angles, which define the range of the day/night switch. The minimum and maximum solar zenith angles depend on the altitude.

$$\theta_{\min} = [90.57 + 0.123(alt - 50)] - 2.5 \text{ and } \theta_{\max} = [90.57 + 0.123(alt - 50)] + 2.5 \tag{3}$$

where *alt* is the altitude (km) and the terms in the square brackets are linear fits to the 50% point solar zenith angle. The factor of 2.5 provides a 5 degree range and the factor of 0.123 causes the midpoint of the interpolation region to vary at a rate of 0.123° per km. W approaches or equals 0 during the night and 1 during the day, and is set to 0 during continuous polar nighttime and 1 during continuous polar daytime.

For $CO_2$ and NO, W is calculated with the assumptions that the approach to the daytime or nighttime equilibrium starts immediately at sunrise or sunset (SZA = 90°) and proceeds with a characteristic time constant, $\tau$. An analytical solution to $W(T_{Rise}, T_{set}, T_{LST})$ exists in this case,

$$W(T_{Rise}, T_{Set}, T_{LST}) = \begin{cases} 1 + (W_r - 1)e^{\tau_d^{-1}(T_{Rise} - T_{LST})} & \text{if } T_{Rise} < T_{LST} < T_{Set} \\ W_s e^{\tau_n^{-1}(T_{Set} - T_{LST})} & \text{if } T_{LST} \geq T_{Set} \\ W_s e^{\tau_n^{-1}(T_{Set} - T_{LST} - 24)} & \text{if } T_{LST} \leq T_{Rise} \end{cases} \quad (4)$$

where $W_s$ and $W_r$ are the values at sunset and sunrise, $T_{LST}$ is the local standard time, $T_{Rise}$ is the sunrise time, $T_{Set}$ is the sunset time, $\tau_n$ is the night time constant, and $\tau_d$ is the day time constant ($\tau_d = \tau_n = 3$ for NO and $\tau_d = \tau_n = 8$ for $CO_2$). Here,

$$W_r = \left( \frac{e_n(1 - e_d)}{1 - e_d e_n} - 1 \right), \quad W_s = \left( \frac{1 - e_d}{1 - e_d e_n} \right) \quad (5)$$
$$e_d = e^{-(T_{Set} - T_{Rise})/\tau_d}, \quad e_n = e^{-(24 - (T_{Set} - T_{Rise}))/\tau_n}$$

In calculating the sunrise and sunset LST's, 0° longitude is assumed. This can lead to a small error, typically less than one minute, compared to the sunrise and sunset times at the actual longitude.

### 3.1 SHARC Species

#### 3.1.1 $CO_2$

The $CO_2$ profile is computed from specified nighttime and daytime ratios relative to the argon number density, which is obtained from MSISE-90/NRLMSISE-00. Below 90 km, a fixed $CO_2$/Ar ratio is used, based on a ground level $CO_2$ mixing ratio of 340 ppm. Above 90 km, the ratio decreases, and separate daytime and nighttime equilibrium ratios are used. These daytime and nighttime $CO_2$/Ar ratios were obtained by combining the theoretical calculations of Rodrigo *et al.*[12] for sunrise (representing nighttime equilibrium) and sunset (representing daytime equilibrium) with mass spectrometric measurements. MSISE-90 was used to compute Ar

densities corresponding to the conditions of Rodrigo *et al.*[12]; using their $CO_2$ densities, the $CO_2$/Ar ratios were taken. These ratios were then systematically rescaled for overall consistency with measurements from the daytime Aladdin experiment[13] and lower-altitude nighttime measurements.[14] For $CO_2$ diurnally dependent interpolating factors are defined at 120 km and 150 km,

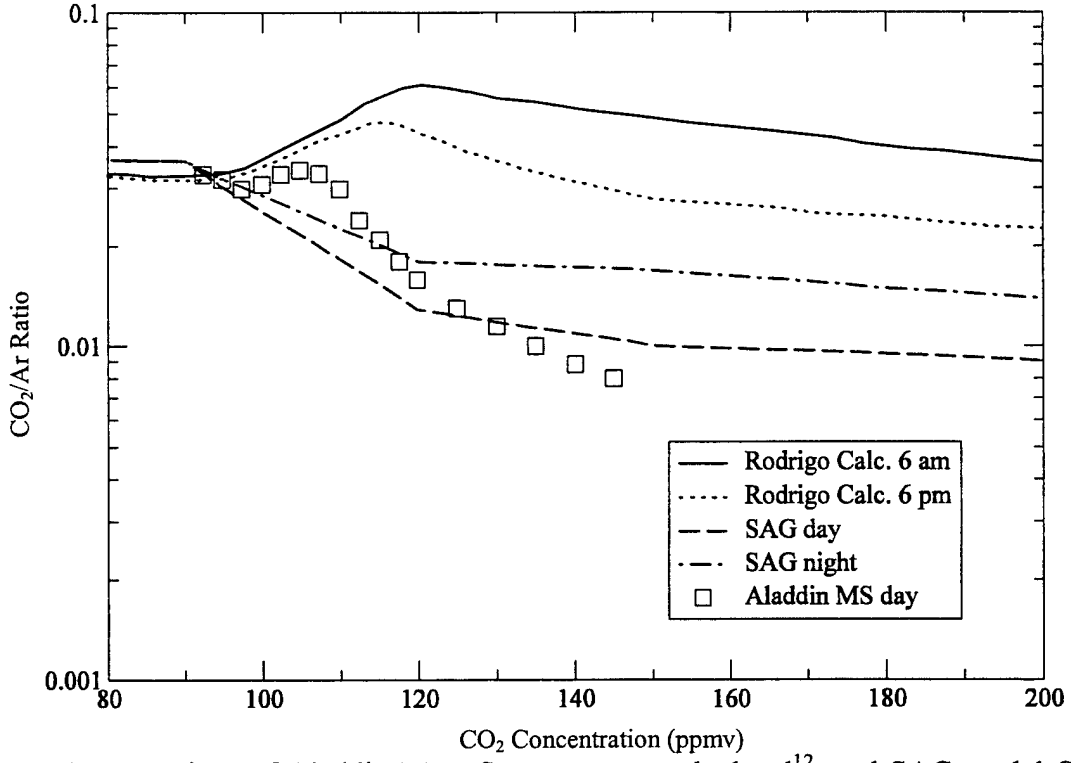


Figure 2: A comparison of Aladdin Mass Spectrometer, calculated[12], and SAG model $CO_2$/Ar density ratios.

$$X_{120} = \mathrm{LOG}(0.013W + 0.18(1 - W)) \text{ and } X_{150} = \mathrm{LOG}(0.010W + 0.17(1 - W)) \qquad (6)$$

where $X_{ht}$ is the $CO_2$/Ar ratio at an altitude of *ht* km. The value of W is determined from equation 4 with a relaxation time constant $\tau$ of 8 hrs for both day and night. The $CO_2$ density is then given by,

$$\begin{aligned}
[CO_2] &= [Ar]X_{90} && \text{for alt} < 90 \text{ km} \\
[CO_2] &= [Ar]e^{((X120(alt-90) + X90(120 - alt))/30)} && \text{for } 90 \text{ km} \le \text{alt} < 120 \text{ km} \\
[CO_2] &= [Ar]e^{((X150(alt-120) + X120(150 - alt))/30)} && \text{for } 120 \text{ km} \le \text{alt} < 150 \text{ km} \qquad (7) \\
[CO_2] &= [Ar]e^{((X300(alt-150) + X150(300 - alt))/150)} && \text{for } 150 \text{ km} \le \text{alt}
\end{aligned}$$

The resulting daytime and nighttime ratios are shown in Figure 2 along with the theoretical calculations and the Aladdin measurements. $CO_2$ concentration profiles generated by this model, such as the examples in Figure 3, are found to be consistent with measurements summarized in a recent review,[15] and are very similar to mid-latitude profiles used previously for IR radiation modeling.[15, 16] New $CO_2$ concentrations have been derived from ATMOS data[17] at altitudes of up to 120 km. The model is found to provide an excellent representation of the average of these somewhat scattered measurements. From these comparisons, the SAG $CO_2$ profile is estimated to be accurate to within ±30% or better in the 100-150 km range.

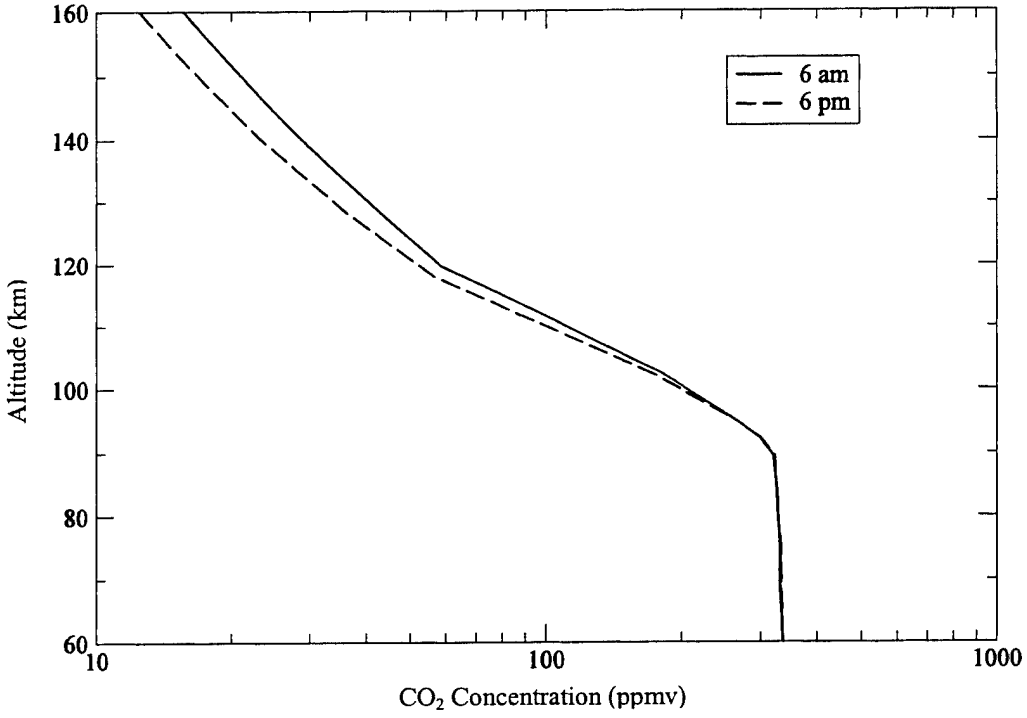


Figure 3: The SAG 2.0 $CO_2$ concentration profiles for autumn, mid-latitude, and moderate-activity conditions.

### 3.1.2 NO

Updates to the NO profile based on the SNOE database may be included from the Parameter Menu (see Table 1). When the SNOE database is not used then the NO profiles from SAG version 0.92 are obtained.

*SAG 0.92 NO Profiles*

Below 90 km, the NO concentration is taken from the AFGL Constituent Profiles tabulation.[11] While the actual concentration should have strong diurnal and latitude variations, little or no NO radiation is expected to be observable from this altitude range due to competing sources. At higher altitudes, NO emission is quite strong, so the variations need to be modeled. Above 100 km, separate daytime and nighttime profiles are calculated from the empirical latitude, temperature, and Kp-dependent models of Smith et al.,[18] as discussed below. The time

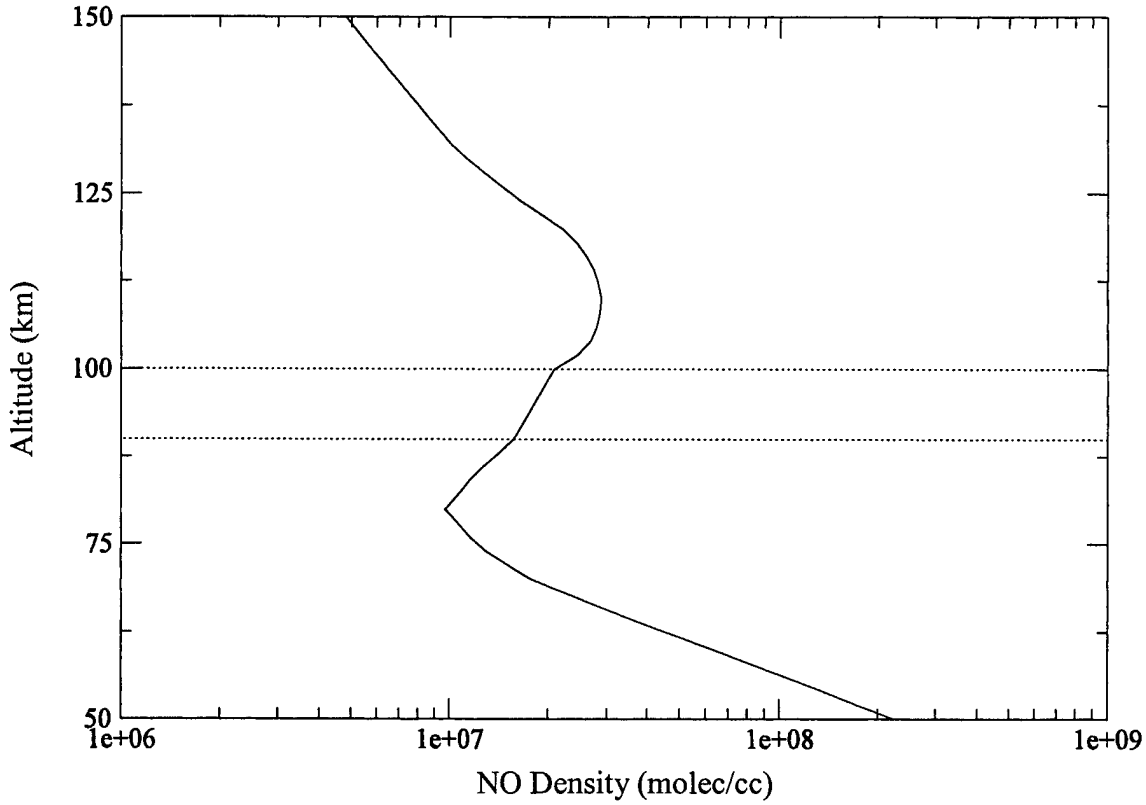


Figure 4: A plot of the mid latitude daytime NO profile showing the density interpolation. The altitudes 90 km and 100 km are marked with dotted lines.

constant $\tau$ is taken as 3 hours. The densities between 90 and 100 km are estimated by interpolation (Figure 4). Therefore, for 90 km and higher the NO density is given by,

$$[NO] = [NO_{90}]^{0.1(100-alt)}[NO_{100}]^{(1-0.1(100-alt))} \text{ for } 90 \text{ km} \leq alt \leq 100 \text{ km} \quad (8)$$

$$[NO] = W[NO_{day}] + (1-W)[NO_{night}] \text{ for } 100 \text{ km} < alt \quad (9)$$

where W is from equation 4, $[NO_{90}]$ is the NO number density at 90 km calculated from the MODTRAN database, $[NO_{100}]$ is the NO number density at 100 km, $[NO_{day}]$ is the daytime NO profile, and $[NO_{night}]$ is the nighttime profile. The daytime and nighttime profiles were chosen to give consistency with the latitude-dependent diurnal variation in NO reported by Smith et al. and with low-latitude satellite measurements[19] during daylight hours. The nighttime profile above 100 km is specified using a fitting parameter, the so-called equatorial night/day ratio $NO_e(n)/NO_e(d)$, which is given an altitude-dependent value of between 0 and 0.2. This ratio is a fictitious quantity since the minimum latitude absolute value for the NO computation is taken to

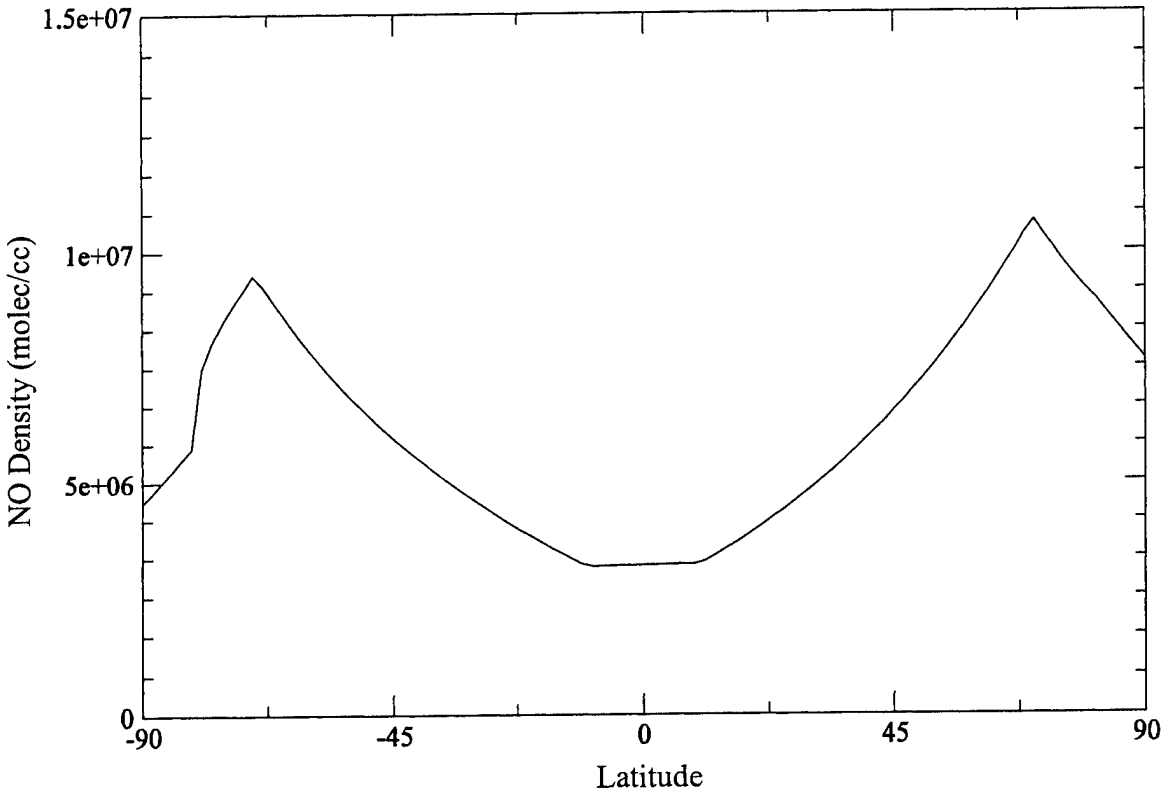


Figure 5: A plot of the nighttime NO density as a function of latitude for SAG 0.92 at 110 km. For latitude absolute values > 70° the latitude is "folded back" to give better agreement with satellite data.

be 10°, to ensure that finite values of nighttime NO are obtained at the equator. For latitude absolute values > 70°, the latitude is "folded back" (i.e. effective latitude = 140-lat, see Figure 5) to give better agreement with satellite data compiled by Barth.[20] Taking average nighttime and

daytime NO densities as represented by LST = 0 and 12 hr respectively, the results at 110 km are in reasonable agreement with the data compiled by Smith et al.[18]

The time-dependent behavior of NO according to this empirical model is shown in Figure 6. The low-latitude simulation reasonably reproduces the increase in mesospheric NO at sunrise found in the Atmospheric Explorer C measurements.[19] However, it predicts the maximum to occur at sunset, whereas the observed maximum is somewhat earlier, in the mid-afternoon. The nighttime behavior of NO at low latitudes is not known from measurements, as the satellite data are from a solar fluorescence technique and there have been very few rocket measurements at low latitudes. Available IR measurements [18] show little diurnal variation at polar latitudes.

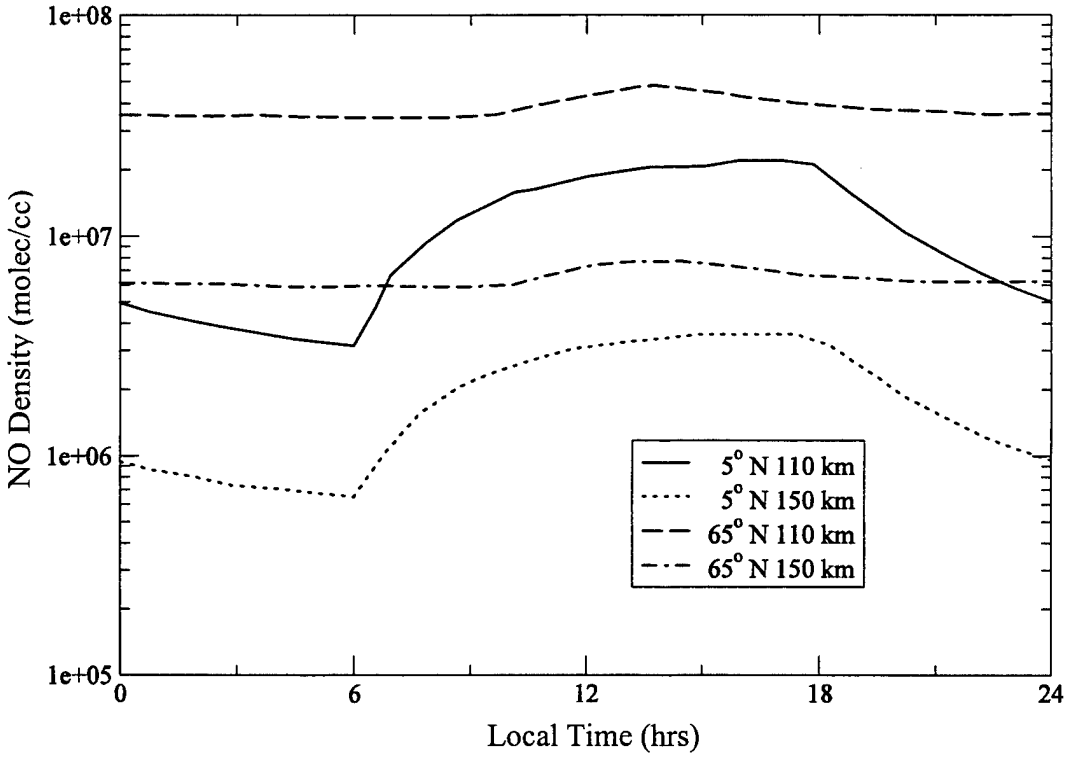


Figure 6: The diurnal dependence of NO densities for autumn with moderate-activity conditions.

### *SAG 2.0 NO Profiles*

If the SNOE database option is chosen then an NO density profile based on the SNOE database is smoothly integrated into the existing SAG profile for altitudes between 97 km and 150 km. The SNOE data were averaged to produce a database that gives the NO density as a

function of altitude and latitude for each month. The density dependence on Ap index is determined by correlating the SNOE density against an Ap index database.[21] Variation in density as a function of Ap index was fit via linear least squares at specific altitudes. These fits were then used to generate a scaling factor for the average NO density, which is a function of altitude and Ap index (see Figure 7). The magnitude of the diurnal variation is taken from the SAG 0.92 profiles and used to scale the SNOE data. A comparison of the NO profiles for SAG with and without the SNOE database is shown in Figure 8.

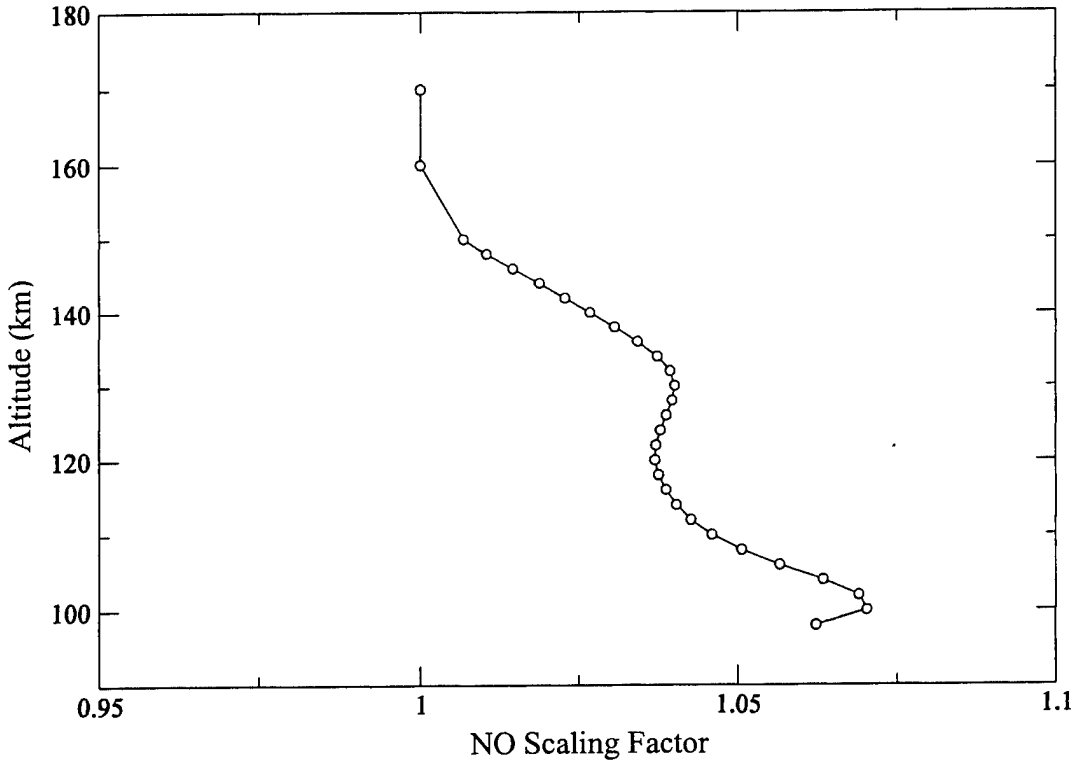


Figure 7: The NO scaling factor for an Ap index of 15.

### 3.1.3 O Atoms

An option to scale and augment the O atom profiles to improve agreement with experimental measurements has been added to the Parameter Menu (see Table 1). These updates may be used with either MSISE model. When MSISE-90 is used without the updates, the O atom profiles from SAG version 0.92 are obtained.

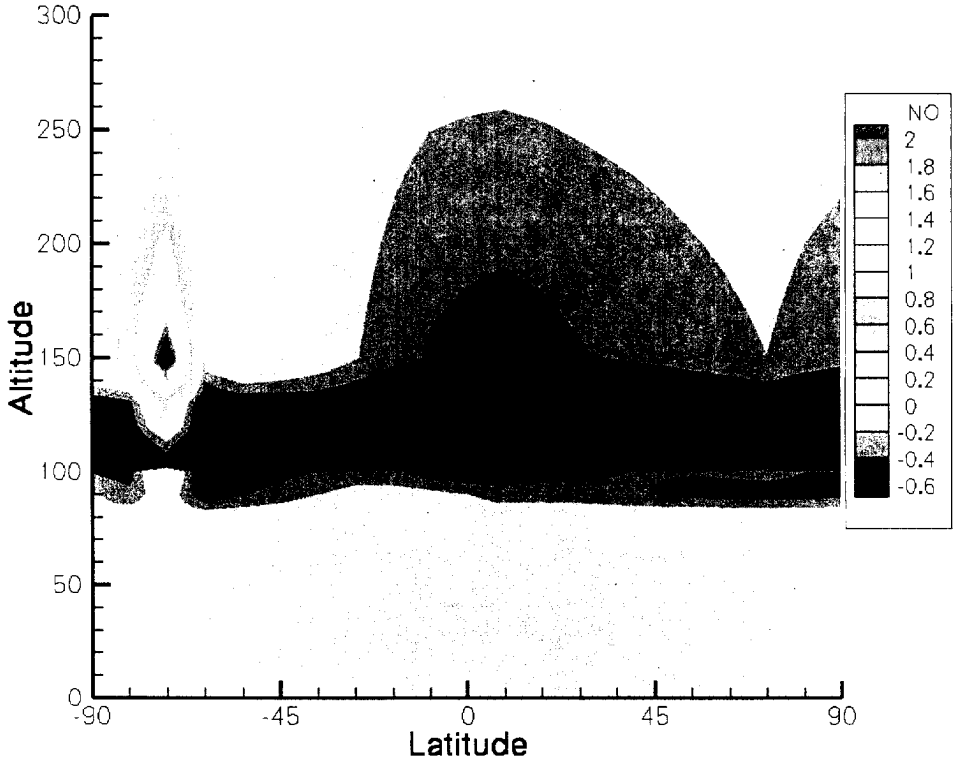


Figure 8: Nitric oxide number density differences between SAG 0.92 and SAG 2.0 using NRLMSISE-00 and SNOE for noon, spring, mid-latitude, and moderate-activity conditions. The figure shows the relative difference: $([NO]_{0.92} - [NO]_{2.0})/[NO]_{2.0}$, where [NO] is the nitric oxide number density and the subscript indicates the SAG version. The differences shown below 97 km are due to using different MSISE models when converting from mixing ratios.

***SAG 0.92 O Atom Profiles***

The O atom profiles are adopted from MSISE above 86 km altitude. However, at lower altitudes they are unrealistic, as they lack a diurnal variation. Alternative approaches were therefore used for the lower altitudes.

From 72 to 86 km, daytime and nighttime profile shapes, scaled to the value at 86 km, were estimated from various measurements and calculations in the literature. The nighttime profile is essentially equivalent to that of the U.S. Standard Atmosphere. Below 72 km, the daytime O atom profile is computed from the daily average value from the NRL climatology database[3] under the assumption that the nighttime value is zero; the day length is accounted for. The result is rescaled to match the lower boundary of the 72-86 km region daytime profile. The scale factor, which is typically between 0.6 and 1.6, is reported to the user. The O atom profiles are

switched from day to night using the linear interpolation scheme of the ozone terminator model, discussed in the following subsection. In particular:

$$\begin{aligned} [O] &= W[O]_{day} + (1-W)SO_{night}[O]_{86} && \text{alt} = 72 \text{ km} \\ [O] &= W \times SO_{day}[O]_{86} + (1-W)SO_{night}[O]_{86} && 72 \text{ km} < \text{alt} < 86 \text{ km} \\ [O]_{day} &= [O]_{NRL} \frac{[O]_{D72,MSIS}}{[O]_{D72,NRL}} \times \frac{12}{T_{Rise}} \end{aligned} \qquad (10)$$

where the SO parameters are scaling factors for the shape of the O profile.

The predicted O atom profiles should be reasonable at most altitudes during the day, when the concentration is nearly in steady state, but almost meaningless for altitudes below 80 km at night, when the concentration drops rapidly. Fortunately, such low O atom concentrations are believed to have little impact on atmospheric IR radiation.

***SAG 2.0 O Atom Profiles***

An updated O atom profile may be derived from either of the MSISE models. The O atom profile was empirically modified to be in better agreement with experimental measurements[22-28,32], while retaining diurnal variability. This was done by slightly reducing the MSISE density by scaling with a non-linear function of altitude near the peak density.

$$[O] = [O]_{MSISE}\left(S + (1-S)(\text{abs}(\text{alt} - \text{alt}_{max})/d)^2\right) \qquad \text{for } \text{alt}_{max} - d < \text{alt} < \text{alt}_{max} + d \qquad (11)$$

where $[O]_{MSISE}$ is the MSISE oxygen density, $S = 0.875 - C(1 - D_n)$ is a scaling factor, $C = 0.2$ for MSISE-90 and $C = 0.3$ for NRLMSISE-00, $\text{alt}_{max}$ is the altitude at the MSISE maximum oxygen density, $D_n$ controls the diurnal variability, and d (= 25 km) controls the scaling width. The density is augmented by adding the lower peak to better reproduce the O atom profile and diurnal variability,

$$[O] = [O]_{max} D_n e^{\left(-4\ln(2)((\text{alt}-(\text{alt}_{max}-\text{alt}_{peak}))/(\text{FWHM}))^2\right)} \qquad \text{for alt} < \text{alt}_{max} \qquad (12)$$

where $[O]_{max}$ is the maximum in the MSISE density profile located at an altitude $\text{alt}_{max}$, FWHM is the full width at half max of the distribution, and $\text{alt}_{peak}$ is the altitude of the secondary maximum in the oxygen distribution. For Oxygen, the FWHM employed is 22 km for altitudes above the secondary maximum and 34 km for lower altitudes. $D_n$ varies from 1.0 to 0 (day to night). Comparisons of the original and updated densities are shown in Figure 9 and Figure 10.

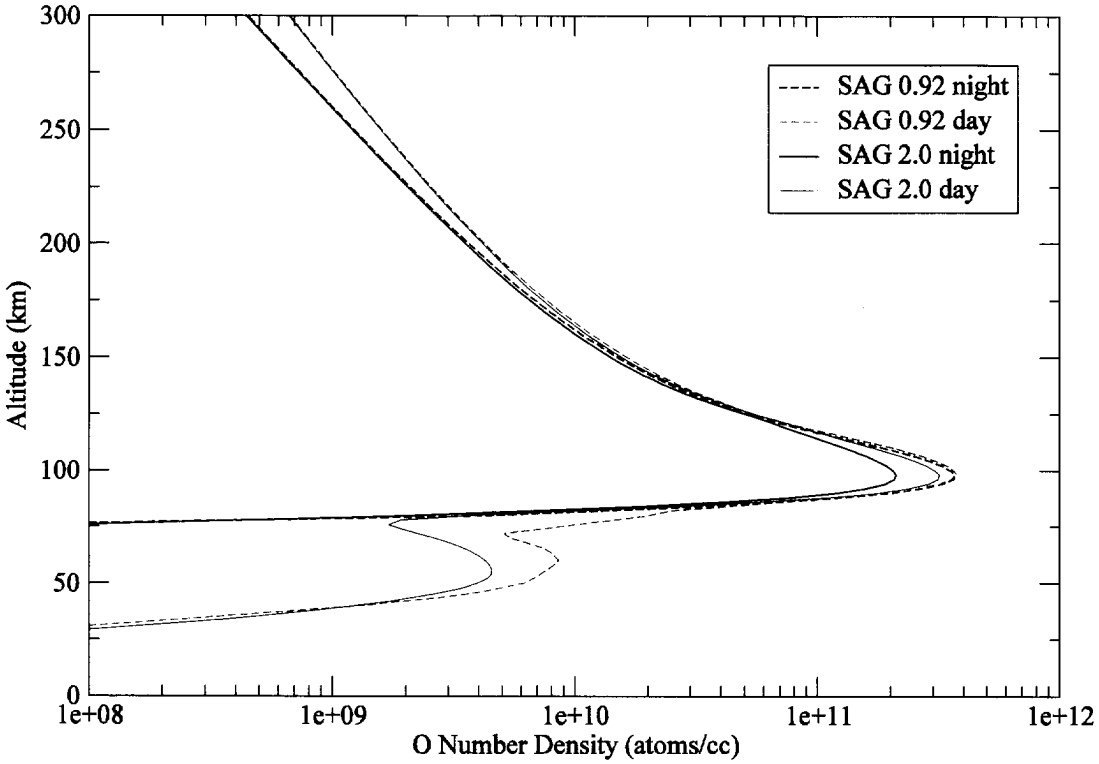


Figure 9: A comparison of the original and updated O atom density profiles for mid latitude summer.

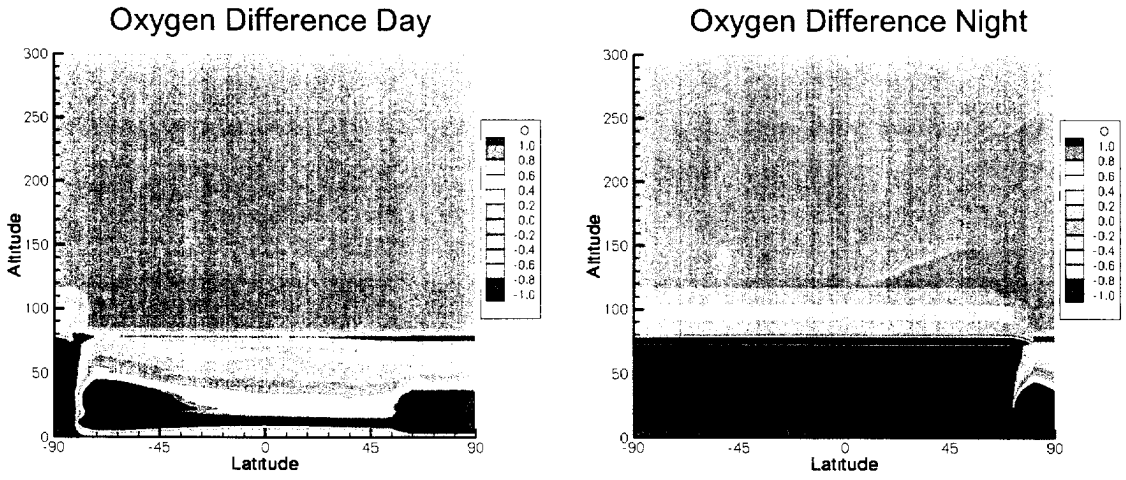


Figure 10: Oxygen number density differences between corrected and uncorrected profiles using MSISE-90 for spring, mid-latitude, and moderate-activity conditions. The figure shows the relative difference: ([O]corrected – [O]uncorrected)/[O]uncorrected, where [O] is the oxygen number density.

### 3.1.4 $O_3$

The ozone profile is presently derived from a combination of the NRL database[3] and a photochemical equilibrium model. The NRL database[3] contains daytime mixing ratios and night/day ratios, and is used below 72 km. The latitude range is restricted to ±60° to avoid difficulties during continuous polar day and night. The photochemical model is used at 80 km and above for MSISE-90 and 82 km and above for NRLMSISE-00. The region between 72 and 80 km (or 82 km) is connected by interpolation.

SAG calculates ozone density above 80 km (or 82 km) using the following photochemical equilibrium model:

$$[O_3] = \{k_1[O][O_2]^2(300/T)^2 + k_2[N_2]\,[O][O_2]\,(300/T)^{2.8} + k_3[O]^2[O_2]\exp(345/T) + k_4[O][O_2]\}$$
$$/\ \{k_5[O]\exp(-2060/T) + k_6[H]\exp(-480/T)\}, \qquad (13)$$

where for the production (numerator) terms, $k_1 = 6.2\times10^{-34}$ $cm^6/(molec^2\cdot sec)$, $k_2 = 5.7\times10^{-34}$ $cm^6/(molec^2\cdot sec)$, $k_3 = 2.2\times10^{-34}$ $cm^6/(molec^2\cdot sec)$, and $k_4 = 8.0\times10^{-21}$ $cm^3/(molec\cdot sec)$; and for the loss terms (denominator), $k_5 = 8.0\times10^{-12}$ $cm^3/(molec\cdot sec)$ and $k_6 = 1.4\times10^{-10}$ $cm^3/(molec\cdot sec)$. The photochemical equilibrium model accounts for ozone formation from O atoms and destruction via H atom and O atom reactions (the former yielding OH) and solar photolysis. Standard rate constants from the literature [12,29] have been adopted. The inputs are the temperature, $N_2$, $O_2$, O, and H profiles and, if daytime, the photolysis rate. As discussed in the following subsection, uncertainty in the H atom profile leads to a comparable uncertainty in the nighttime ozone. A two-body radiative association term is included as a formation mechanism, and has a significant and increasing impact above 100 km. The value of the rate constant, $8x10^{-21}$ $cm^3molec^{-1}s^{-1}$, is estimated from rate constants for formation and relaxation of the $O_2$-O complex[30] and from $\nu_3$ band Einstein coefficients. It is almost certainly an upper limit. However, for systems applications it is safer to overestimate the ozone than to underestimate it. Furthermore, any overestimation from this 2-body channel would be offset by the presence of certain $O_2^* + O_2$ reactions that have been proposed to form ozone[29] but which are not presently included in SAG.

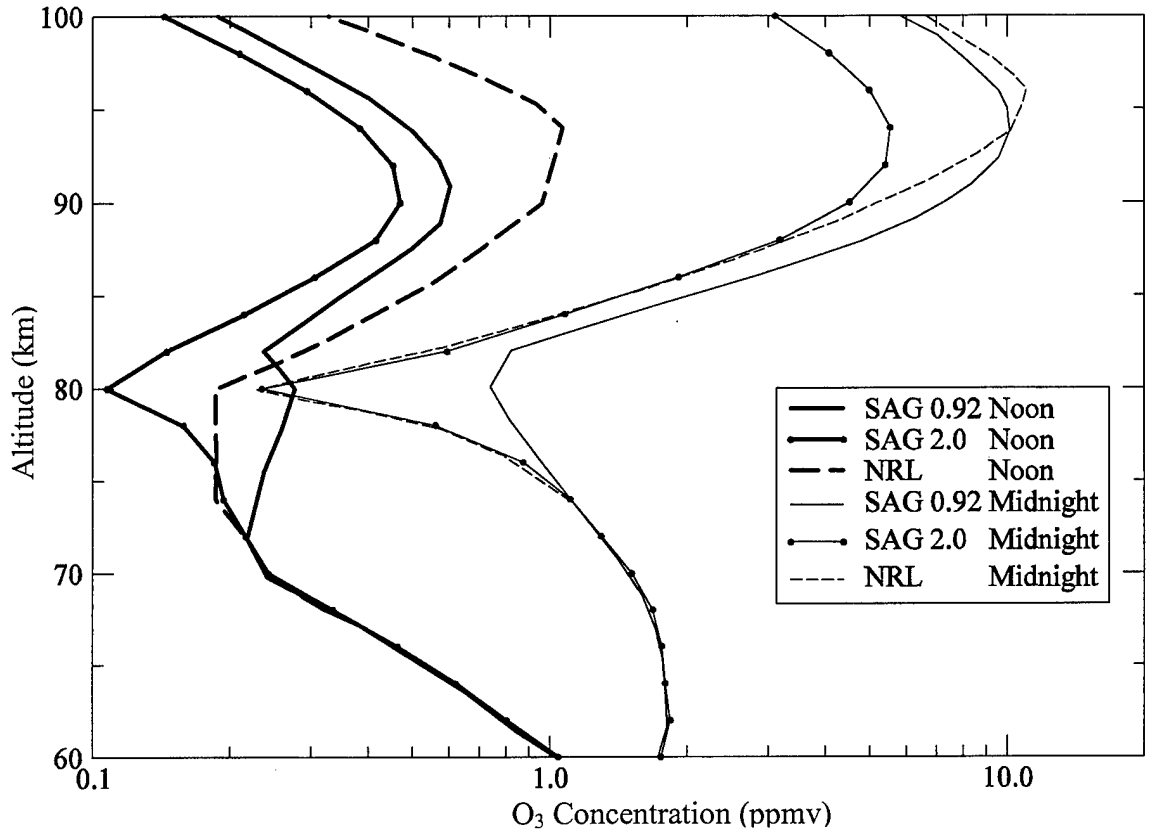


Figure 11: A comparison of the SAG model and NRL climatology ozone concentrations for fall equinox, 45° N, and moderate-activity conditions. Plots for SAG 2.0 include corrections to H atom and O atom densities.

A comparison of typical SAG and NRL ozone concentration profiles is provided in Figure 11. There is quite good agreement between the two, except for the nighttime profile for SAG 0.92 at 80 km. This can probably be ascribed to a slight underestimation of the H atom density at that altitude and by an overestimation of O atom density in SAG 0.92. The new O and H profiles offered by SAG 2.0 (based on either MSISE model) agree much better with the NRL values at 80 km but are consistently lower at 95 km, which brings the subsequent predicted radiances into better agreement with the CIRRIS 1A experiment.[31] A comparison of the calculated ozone density for both MSISE models is shown in Figure 12.

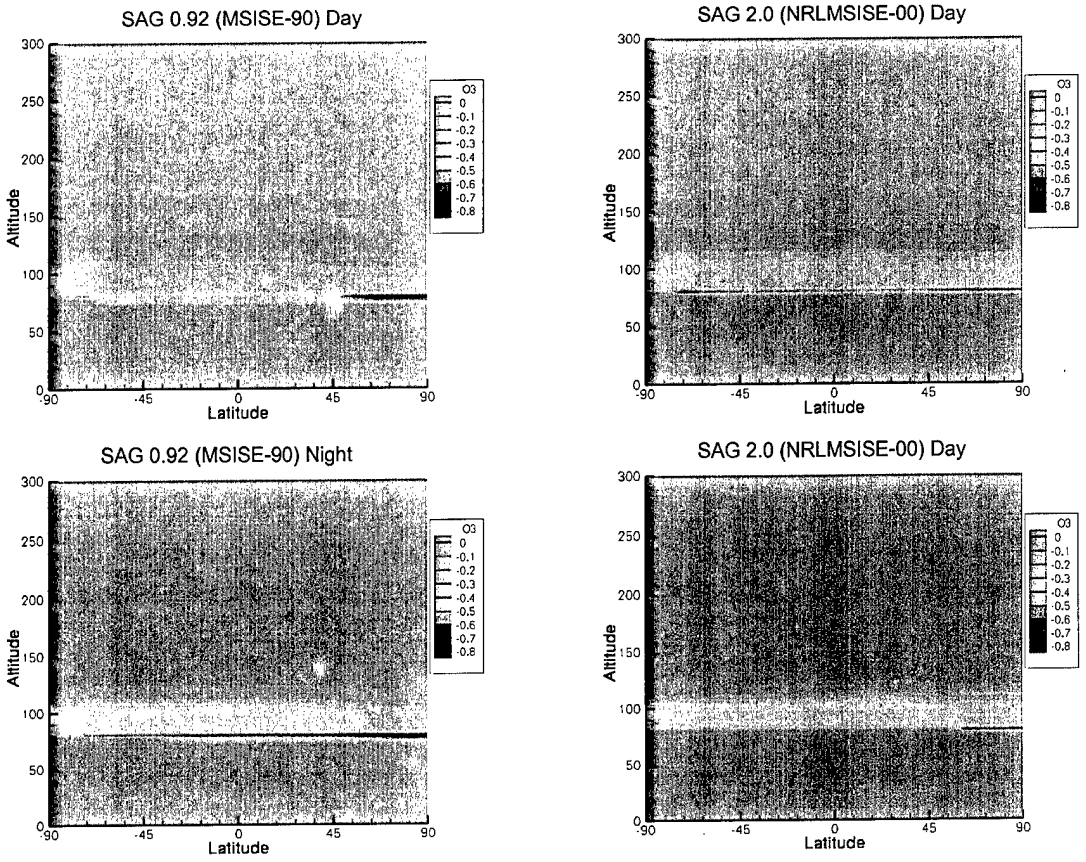


Figure 12: Ozone number density differences for SAG 0.92 and SAG 2.0 with and without H and O corrections for spring, mid-latitude, and moderate-activity conditions. The figure shows the relative difference: $([O_3]_{corr} - [O_3]_{uncorr})/[O_3]_{uncorr}$, where $[O_3]$ is the ozone number density and the subscript indicates the corrected and uncorrected profiles.

The transition between the day and night profiles is handled using a simple empirical model that approximates the terminator behavior in the time-dependent calculations of Rodrigo et al.,[12] which were performed for mid-latitude equinox conditions above 60 km. The transition is made by linearly interpolating over a 5° range of SZA computed for LST-0.075 hr; the 0.075 hr (4.5 min) difference accounts for the approximate photochemical lag time. The midpoint of the interpolation region is taken to vary linearly with altitude at the rate of 0.12° per km. Based on a comparison with Rodrigo et al.'s calculations, this simple representation of the terminator location and width should be accurate to within around 1° in SZA in the 70-100 km altitude

region. Typical time-dependent profiles generated by SAG with MSISE-90 for the dusk terminator are shown in Figure 13.

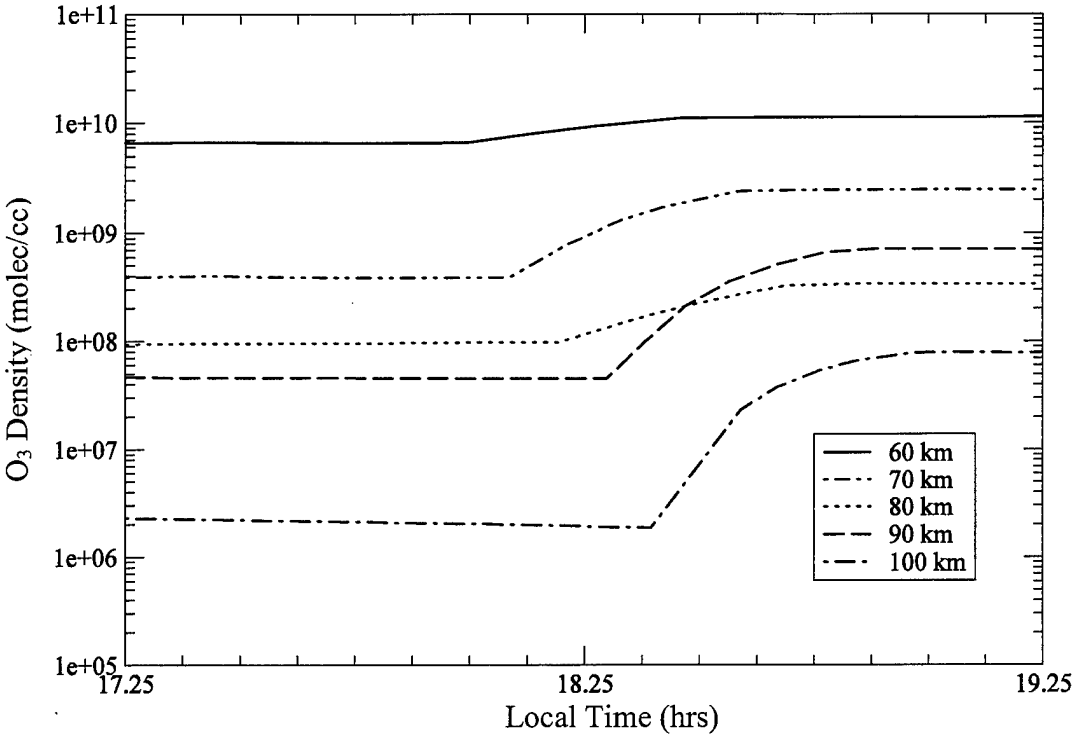


Figure 13: The time-dependence of ozone concentrations at the dusk terminator for fall equinox, 45° N, and moderate-activity conditions.

### 3.1.5 OH

The OH profile is taken from a standard AFGL profile tabulation[11] below 72 km, a chemical equilibrium model above 80 km, and interpolated values in between:

$$WT = (alt - 72)/8 \tag{14}$$

$$[OH] = [OH_{72}]^{(1.0 - WT)}[OH_{80}]^{WT} \qquad \text{for } 72 \text{ km} < alt < 80 \text{ km} \tag{15}$$

$$[OH] = \frac{k_1[O_3][H]\exp(-480/T)}{[O]\exp(-117/T)/k_2} \qquad \text{for } 80 \text{ km} \leq alt \tag{16}$$

where $k_1 = 1.4 \times 10^{-10}$, $k_2 = 2.2 \times 10^{-11}$, $[OH_{72}]$ is the OH number density at 72 km and $[OH_{80}]$ is the OH number density at 80 km. The chemical model, involving formation via the H + $O_3$ reaction and destruction via O atoms, insures that the H, $O_3$, and O concentrations are self-consistent and thus accounts for diurnal variation. The standard profile neglects diurnal variation. Little or no sensitivity of atmospheric radiance to the ground state OH density is

expected, since it neither contributes to nor significantly absorbs the dominant chemiluminescent (Meinel band) radiation from the higher vibrational states.

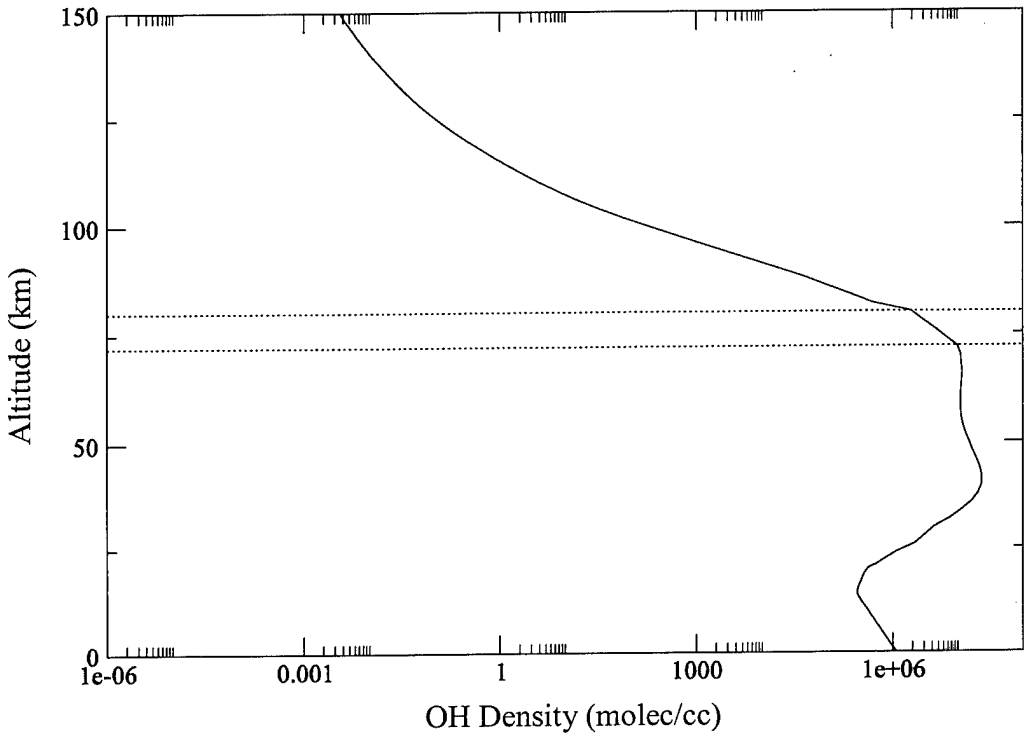


Figure 14: A plot of the mid latitude daytime OH profile showing the density interpolation. The altitudes 72 km and 80 km are marked with dotted lines.

### 3.1.6 H Atoms

An option to scale and augment the H atom profiles based on comparisons with experimental measurements has been added to the Parameter Menu (see Table 1). When these updates are not used then the H atom profiles from SAG version 0.92 are obtained.

***SAG 0.92 H Atom Profiles***

The H atom profile is taken from MSISE-90. As with the O atom profile, the H atom profile cuts off below 74 km, and its accuracy is suspect below 80 km due to the lack of diurnal variation. Compared with the nighttime H atom profiles derived by Thomas[32] for the 80-93 km altitude range, the corresponding MSISE-90 predictions appear to average a factor of 2 to 4 lower. However, the uncertainty in Thomas' values is reportedly a factor of 2, and other experiments [33,34] show better agreement with the MSISE-90 profile.

If the H atom profile was indeed too low, the photochemical model for ozone and OH, implemented at and above 80 km, would predict too much $O_3$ at night and too little OH during

the day. There is some evidence for the first effect at 80 km (see Subsection 3.1.4). However, the daytime $O_3$ and nighttime OH densities are not affected by the H atom density.

***SAG 2.0 H Atom Profiles***

An updated H atom profile may be derived from either of the MSISE models. The H atom profile was empirically modified to be in better agreement with experimental measurements.[35-41,32] A Gaussian distribution of H density, centered at the H peak density, is added to the profile.

$$[H] = [H]_{max}\, e^{\left(-4\ln(2)((alt-alt_{max})/(Dn\times FWHM))^2\right)} \qquad \text{for alt} < alt_{max} \tag{17}$$

where $[H]_{max}$ is the maximum in the MSISE density profile located at an altitude $alt_{max}$, $D_n$ controls the diurnal variability, and FWHM is the full width at half max of the distribution. For Hydrogen, the FWHM employed is 19.5 km and $D_n$ varies from 1.0 to 0.5 (day to night). The value of FWHM and its diurnal variability is chosen to best reproduce experimental data. The supplemental density is used for altitudes up to the H peak density near 85 km. The resulting H atom profiles for MSISE-90 are compared to the unmodified profile in Figure 15.

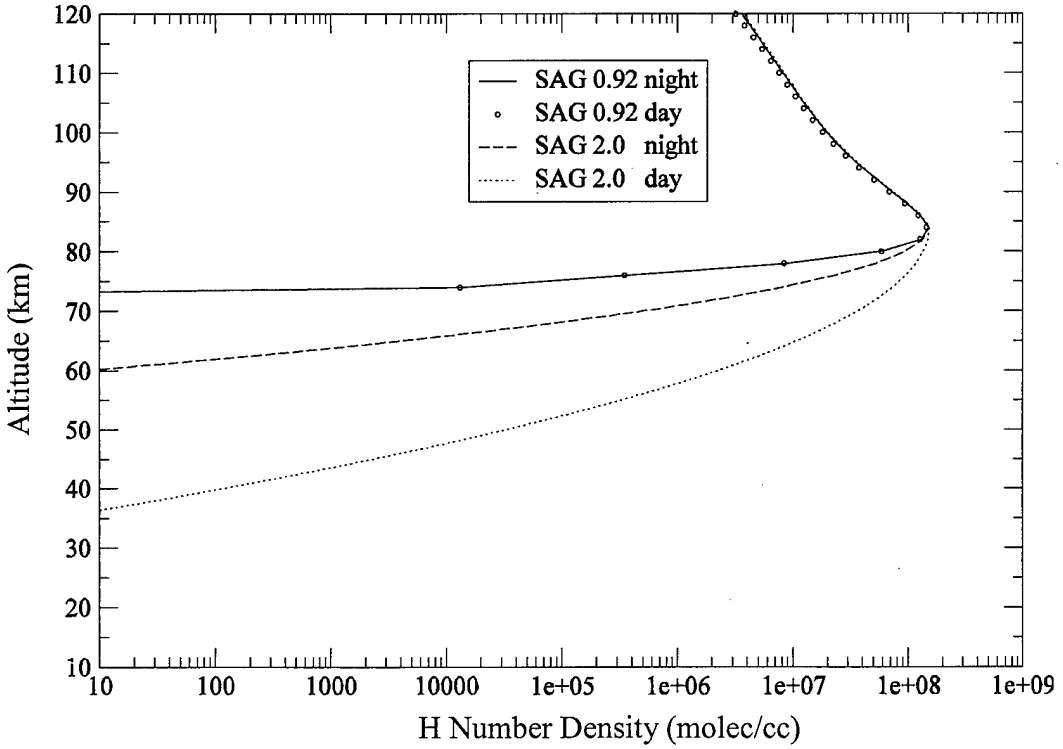


Figure 15: A comparison of the H atom profiles for two versions of SAG for mid latitude summer. The SAG 2.0 profiles are obtained using the H corrections.

### 3.1.7 CO and $CH_4$

The CO and $CH_4$ profiles are taken from the NRL database[3] for altitudes up to 120 km. Above 120 km the mixing ratios are set equal to the 120 km values; this should result in an upper limit to the expected IR radiances, which are extremely small.

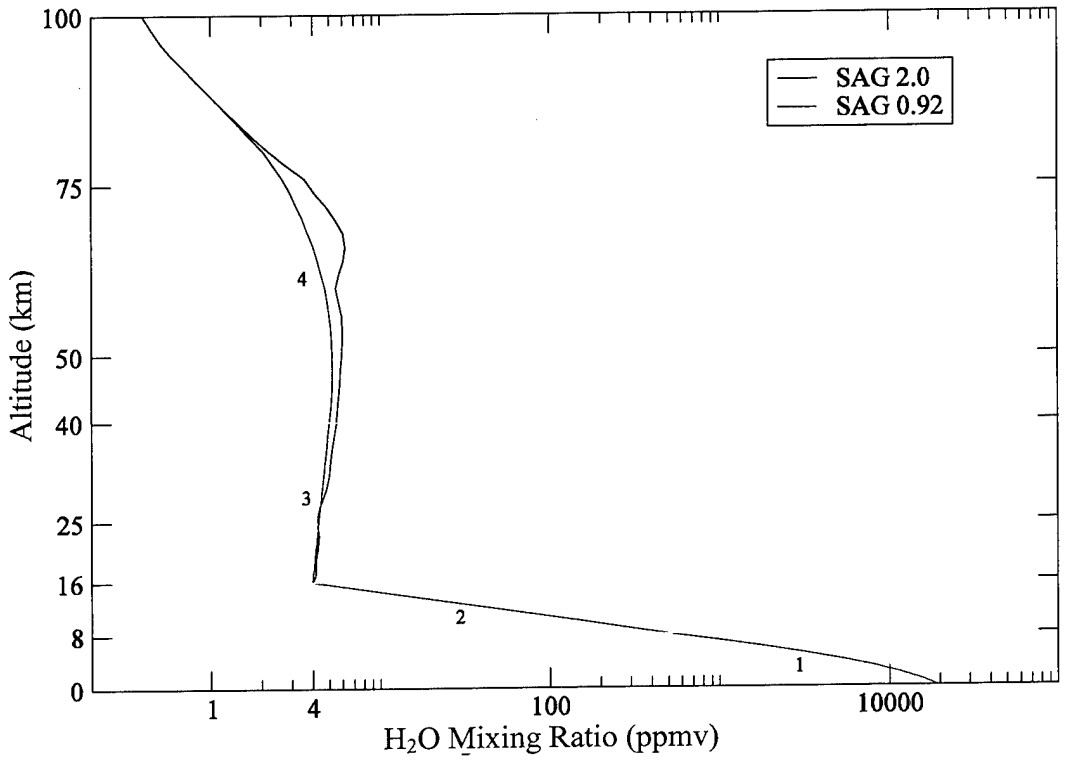


Figure 16: The SAG water vapor profile. The four regions of the profile are numbered.

### 3.1.8 $H_2O$

Updates to the $H_2O$ profile based on the URAP[4] database may be included from the Parameter Menu (see Table 1). When the URAP database is not used then the $H_2O$ profiles from SAG version 0.92 are obtained.

***SAG 0.92 $H_2O$ Profiles***

Due to problems in the current NRL database[3] for water vapor, an alternative empirical model has been developed for SAG which combines the models in Ref. 11 with the recommendation in Ref. 42 for the upper troposphere. Between 0 and 8 km the profile is a linear

fit to the models for relative humidity, which indicate an average humidity of approximately 75% at the ground and 30% at 8 km (Figure 16, region number 1). As recommended in Ref. 42, above 8 km the mixing ratio is logarithmically interpolated to the value of 4 ppmv (2.5 ppmm) at the tropopause, which we take as the altitude of the MSISE temperature local minimum (Figure 16, region number 2). In the unlikely event that the tropopause is below 9 km, it is assumed to be at 9 km for the purposes of this calculation. At 40 km and above, the standard profile from Ref. 11 is used (Figure 16, region number 4). Between the tropopause (4 ppm mixing ratio) and 40 km (approximately 5 ppm mixing ratio) the mixing ratio is logarithmically interpolated (Figure 16, region number 3).

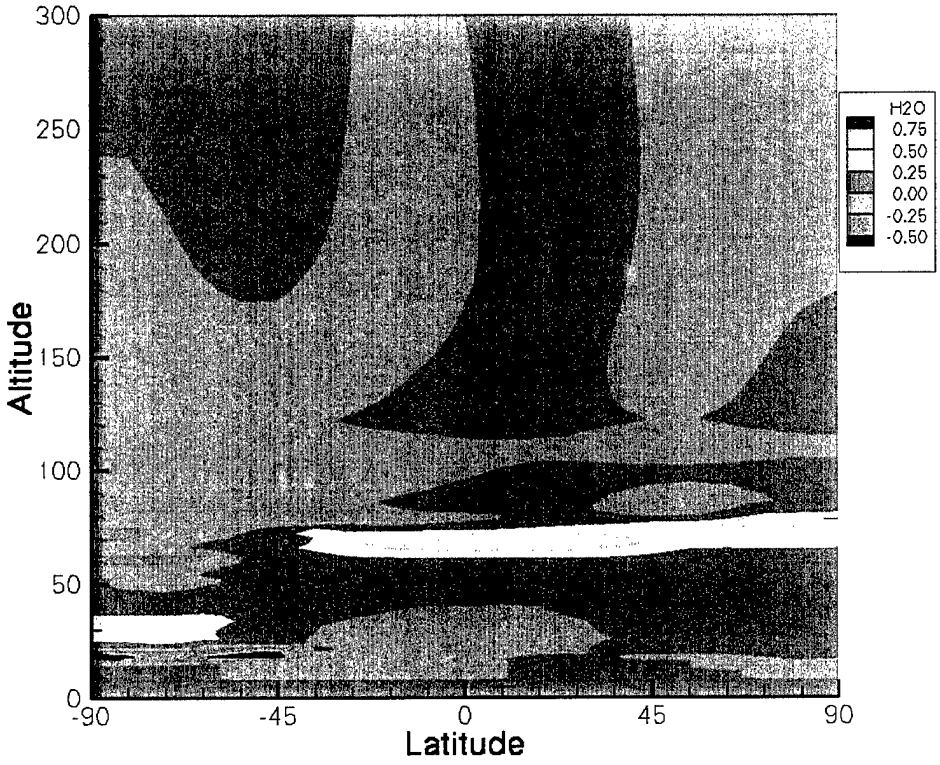


Figure 17: Water vapor number density differences between SAG 0.92 and SAG 2.0 using NRLMSISE-00 and URAP options for spring, mid-latitude, and moderate-activity conditions. The figure shows the relative difference: $([H_2O]_{2.0} - [H_2O]_{0.92})/[H_2O]_{0.92}$, where $[H_2O]$ is the water number density and the subscript indicates the SAG version.

***SAG 2.0 $H_2O$ Profiles***

Updates to the $H_2O$ profile based on the URAP[4] water vapor climatology may be included from the parameter menu (see Table 1). The altitude range of the URAP model is from about 16

km to 85 km. For higher altitudes the standard profile from D. Grantham *et al.*[42] is used. The empirical models employed by SAG for altitudes between 0 km and the tropopause have been retained (Figure 16, numbers 1 and 2). If the URAP water vapor climatology is not selected then the original SAG 0.92 water density profiles are obtained when the MSISE-90 option is selected. A comparison of the SAG 0.92 water vapor density and the updated SAG 2.0 water vapor density using the URAP climatology is shown in Figure 17.

### 3.2 Additional Species for SAMM

The species $N_2O$, $HNO_3$, and $NO_2$ are taken from the NRL database.[3] These profiles include seasonal and latitude variabilities, but do not address the diurnal variability, which in the case of $NO_2$ is very large due to daytime depletion by the $NO_2 + O$ reaction and by photolysis. The species $SO_2$ and $NH_3$ are not covered by the NRL database[3], so the standard AFGL constituent profiles [11] are used.

### 3.3 Temperature

The empirical MSISE model developed by Hedin[1,2] provides a smooth extension of the widely-used MSISE upper atmospheric model to the lower atmosphere. The accuracy of the temperature profiles above 120 km, which are based on mass spectrometer, incoherent scatter and satellite drag data, has been discussed in Hedin's documentation for previous MSISE versions. The temperature profiles in MSISE-90 have been designed to follow standard lower atmosphere climatology compilations quite closely (to within several degrees) under most conditions. A comparison of the MSISE and NRL climatology temperatures is provided in the optional SAG output file "dumpfil.dat" (see Appendix B). In most cases, close agreement is found. The MSISE temperature profiles are probably suitable for most SHARC/SAMM applications. It should be noted, however, that IR radiances can be extremely temperature-sensitive, particularly at low temperatures. One altitude region where the temperature uncertainty may be significant is directly above the mesopause, where there is a steep gradient. A comparison of the calculated temperatures for two MSISE models is shown in Figure 18. From the figure, it is evident that there are significant differences between both the day and night temperature profiles.

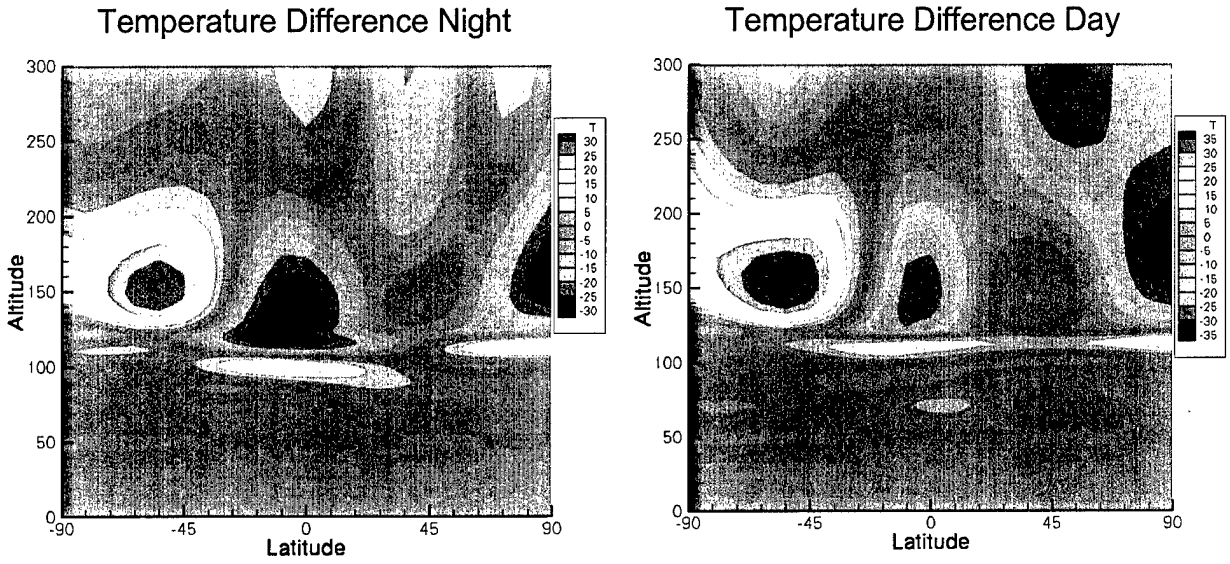


Figure 18: The difference in temperatures between the MSISE-90 and NRLMSIS-00 models for spring, mid-latitude, and moderate-activity conditions. The figure shows the absolute difference: $(T_{NRLMSISE-00} - T_{MSISE-90})$, where T is the temperature and the subscript indicates the MSISE version.

## 4. VERIFICATION AND VALIDATION

SAG atmospheric profiles have been compared to many other profiles from independent sources over a broad range of conditions. A sample of these comparisons for all the chemical species available in SAG is presented here in Figure 19-27. In all of the figures, SAG 2.0 atmospheric profiles are represented by the solid black lines. Comparison of the profiles shows good agreement between the SAG and other profiles.

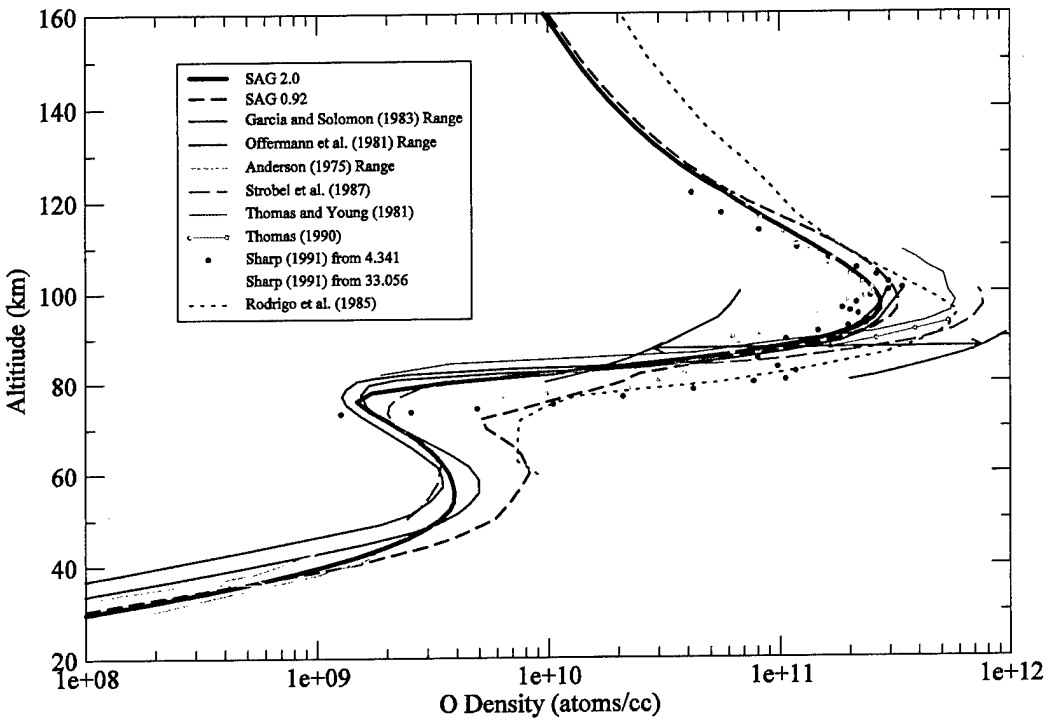


Figure 19: A comparison with SAG daytime, mid-latitude, springtime O atom profiles.

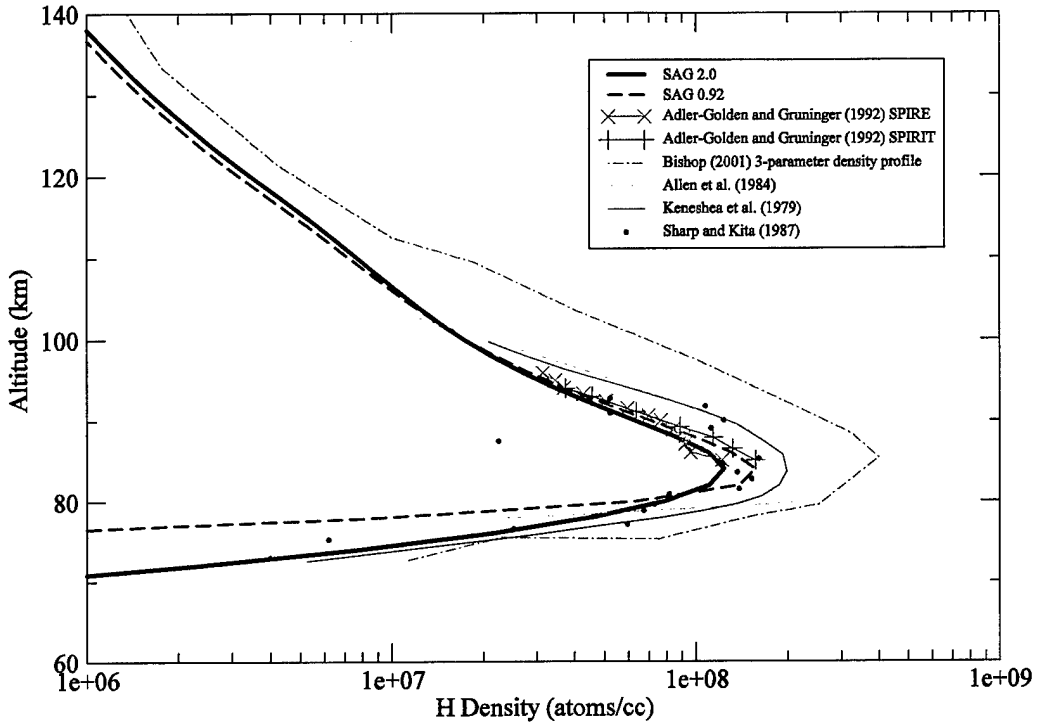


Figure 20: A comparison with SAG nighttime, mid-latitude, springtime H atom profiles.

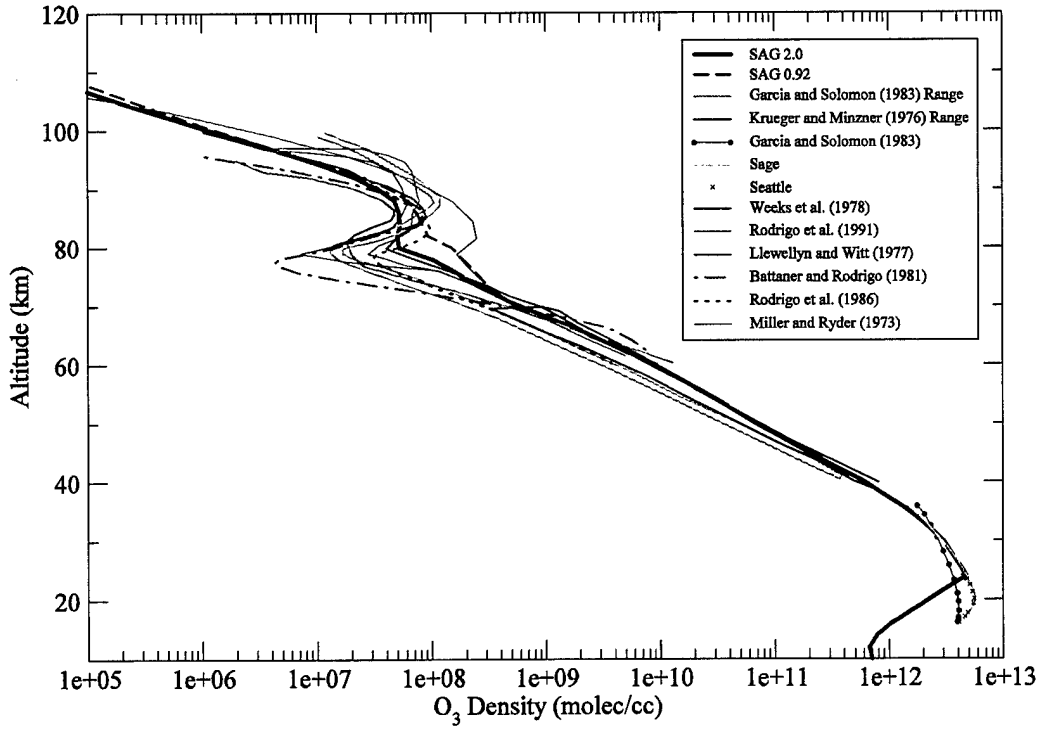


Figure 21: A comparison with SAG daytime, mid-latitude, springtime ozone profiles.

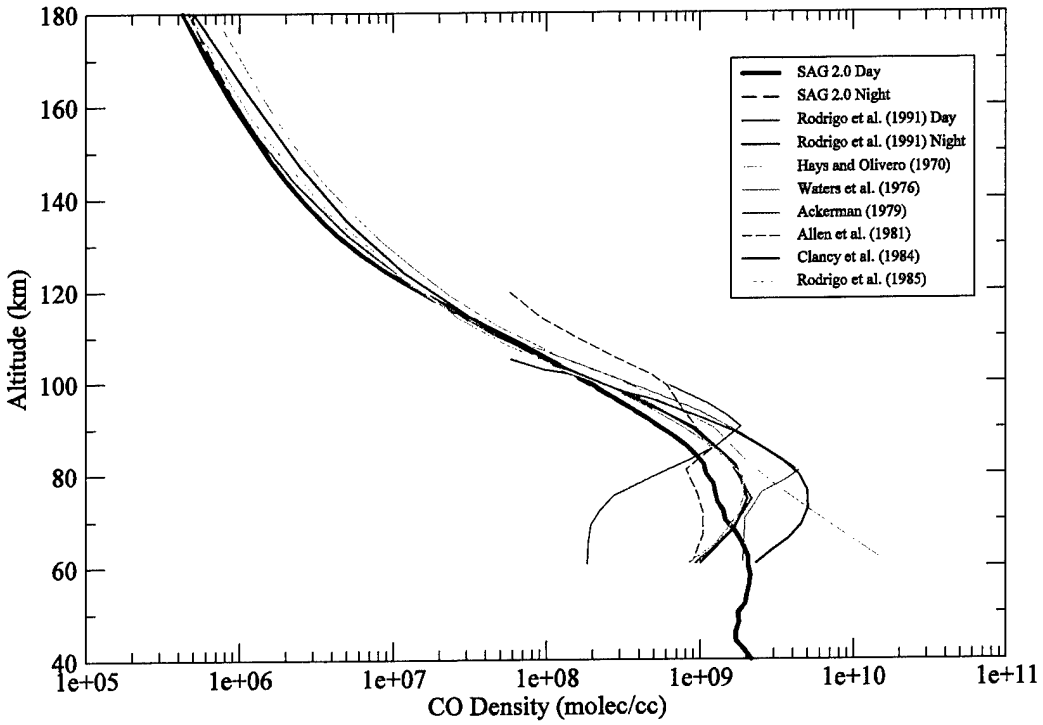


Figure 22: A comparison with SAG mid-latitude, springtime CO profiles.

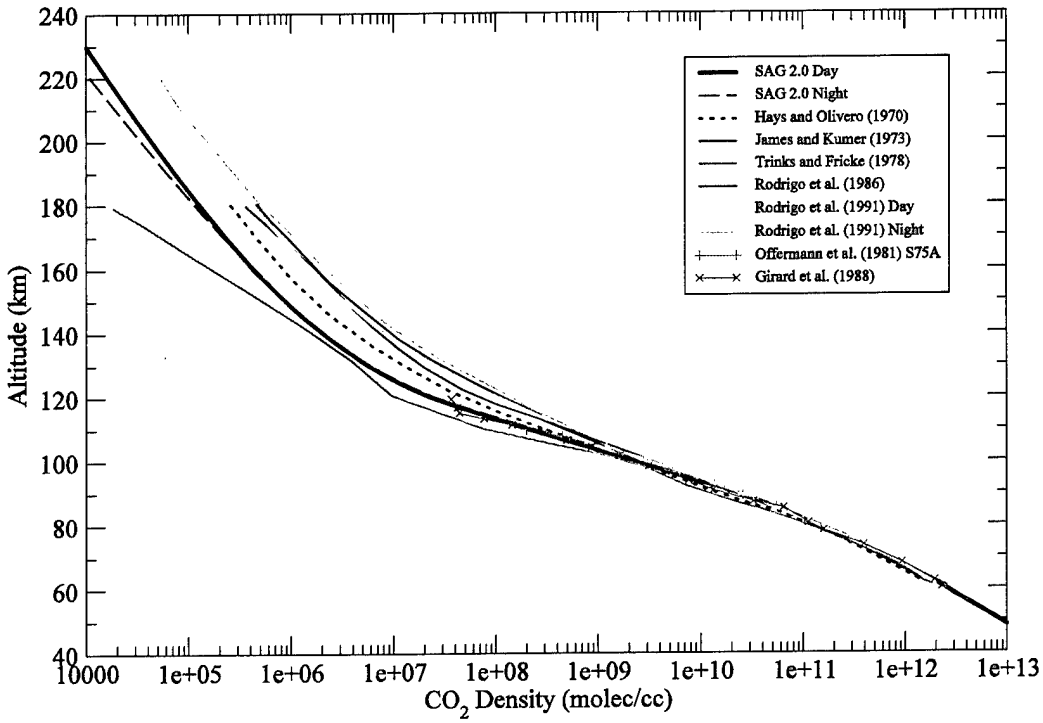


Figure 23: A comparison with SAG mid-latitude, springtime $CO_2$ profiles.

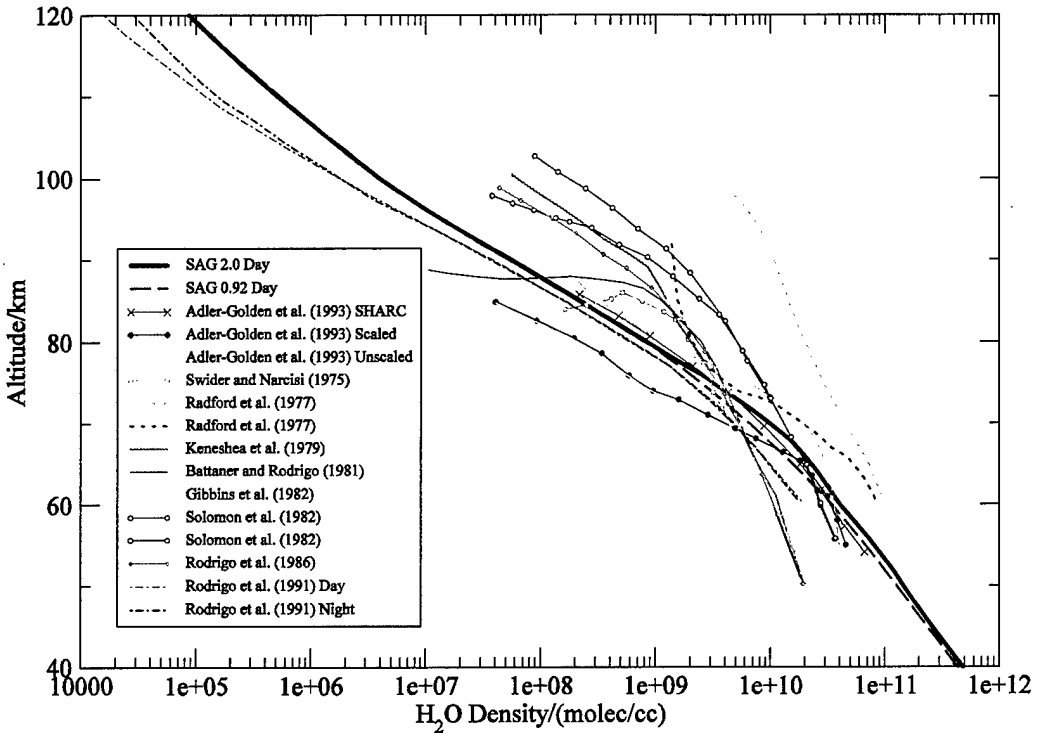


Figure 24: A comparison with SAG mid-latitude, springtime $H_2O$ profiles.

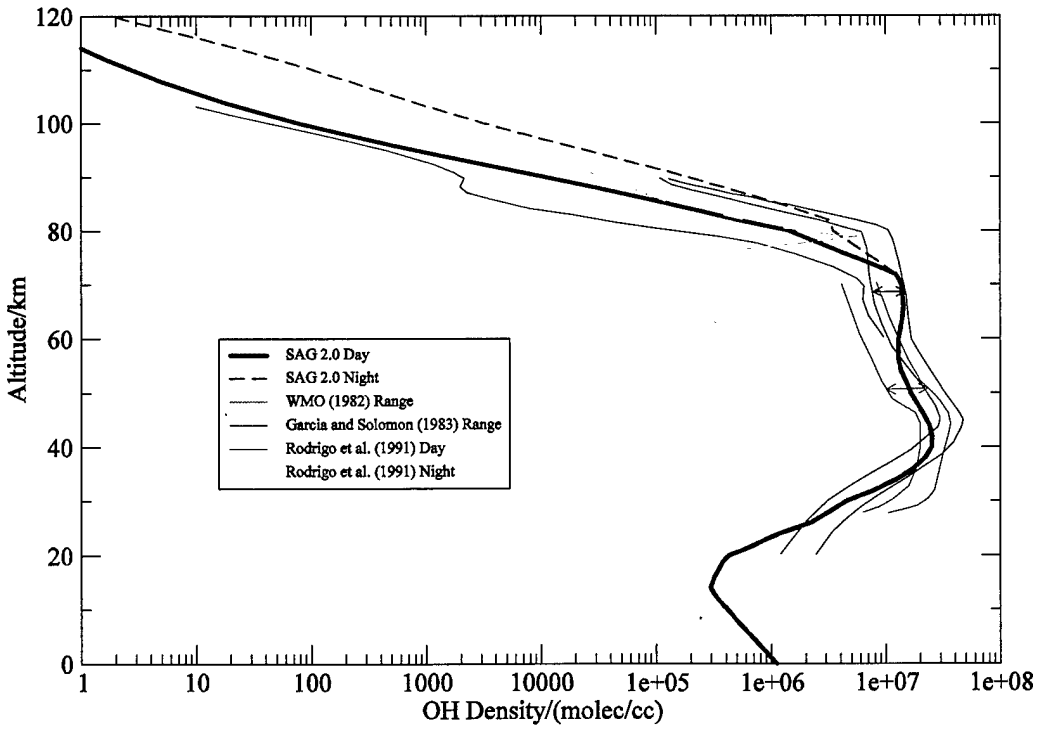


Figure 25: A comparison with SAG mid-latitude, springtime OH profiles.

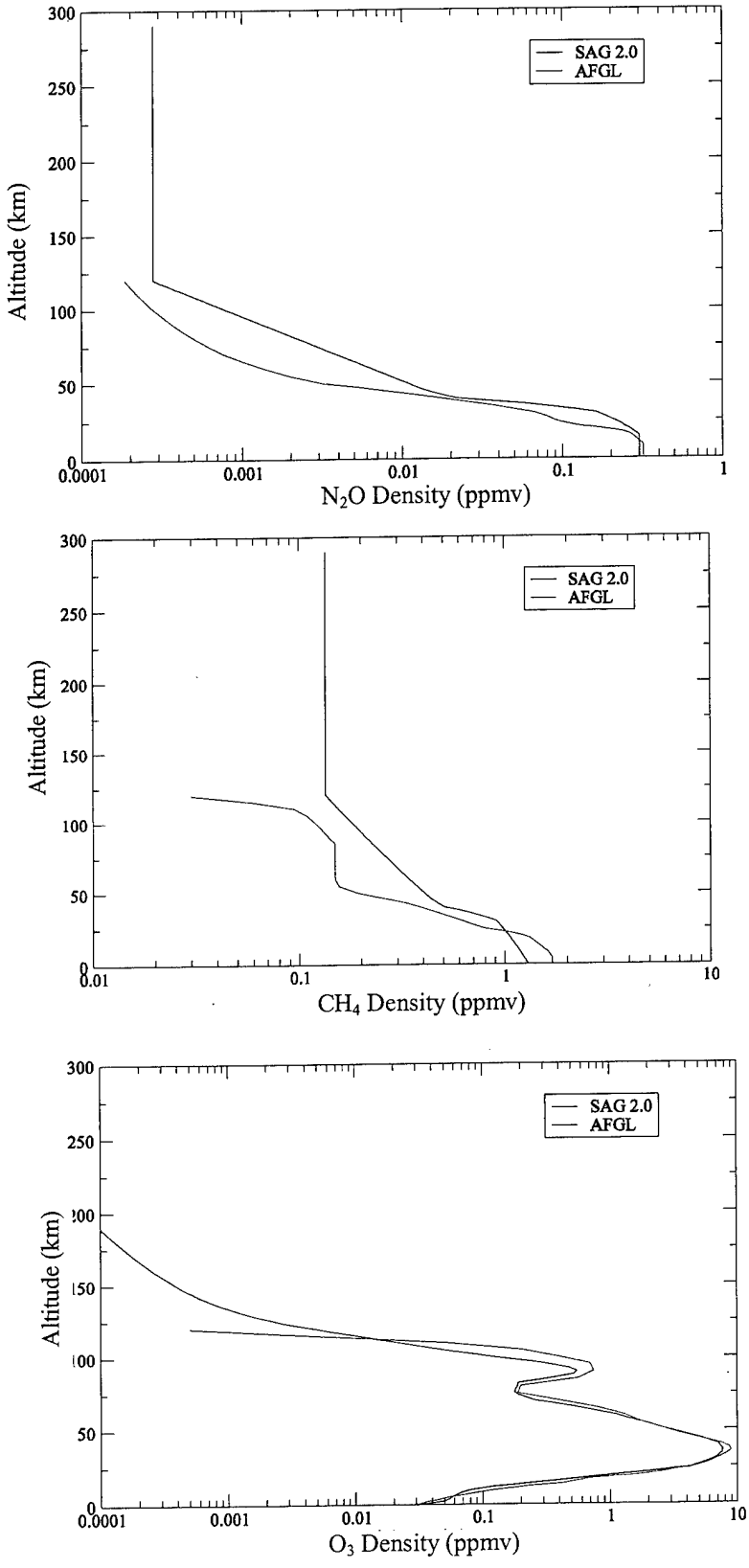


Figure 26: A comparison of SAG and AFGL atmospheric profiles for mid-latitude summer.

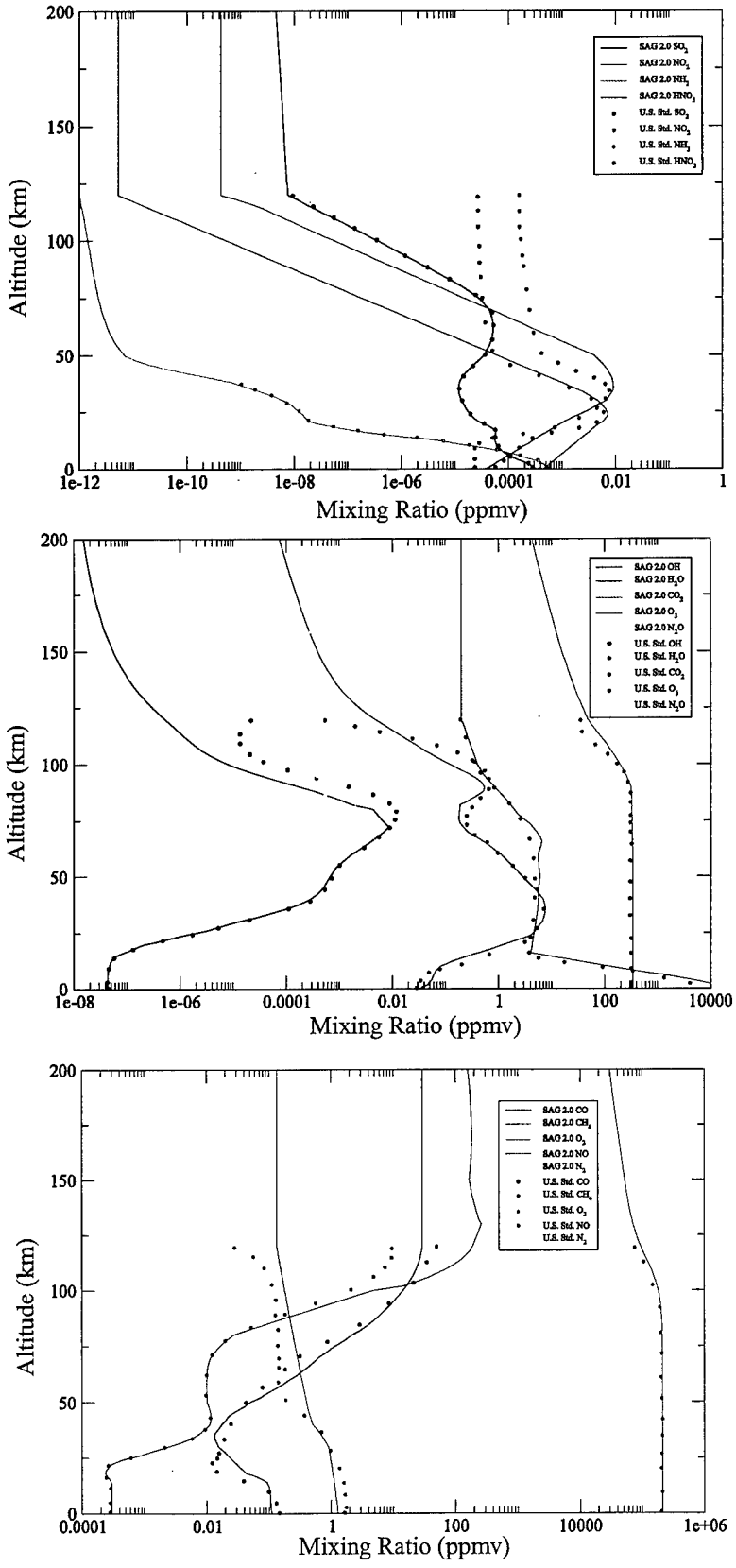


Figure 27: A comparison of SAG and U.S. Standard Atmospheric profiles.

## 5. CONCLUSIONS

The SHARC/SAMM Atmosphere Generator utilizes a combination of empirical models to generate atmospheric profiles for IR radiance calculations that properly account for solar terminator and other systematic variability effects. The goal in developing SAG has been to provide reasonably accurate temperature and species profiles with an easy-to-use, rapid-executing program. It is anticipated that SAG will evolve with the radiation codes to keep up with new observations, theoretical advances, and applications requirements. Comparisons of available field data with radiance predictions will comprise an important parallel effort and will provide valuable tests of the radiation codes and the atmospheric profile models, contributing to our overall understanding of atmospheric processes.

## REFERENCES


1. A. E. Hedin, "Extension of the MSIS Thermospheric Model into the Middle and Lower Atmosphere," *J. Geophys. Res.*, **96**, 1159 (1991).
2. M. Picone, A. E. Hedin, D. P. Drob, and J. Lean, "NRLMSISE-00 Empirical Atmospheric Model: Comparison to Data and Standard Models", AAS/AIAA Astrodynamics Specialist Conference, American Astronautical Society , Paper AAS 01-394, (2001); b) http://uap-www.nrl.navy.mil/models_web/msis/msis_home.htm
3. M. E. Summers, W. J. Sawchuck, and G. P. Anderson, "Model Climatologies of Trace Species in the Atmosphere," Annual Review Conference on Atmospheric Transmission Models, Phillips Laboratory, Hanscom AFB, MA, June, 1992.
4. http://umpgal.gsfc.nasa.gov/uars-science.html
5. J. E. Harries, J. M. Russel, A. F. Tuck, L. L. Gordley, P. Purcell *et al.*, "Validation of Measurements of Water Vapour from the Halogen Occulation Experiment, HALOE," *J. Geophys. Res.*, **101**, 10205, (1996).
6. W. A. Lahoz, M R. Suttie, L. Froidevaux, R. S. Harwood, C. L. Lau, T. A. Lungu, G. E. Peckham, H. C. Pumphrey, W. G. Read, Z. Shippony, R. A. Suttie, J. W. Waters, G. E. Nedoluha, S. J. Oltmans, J. M. Russel III, and W. Traub, "Validation of UARS Microwave Limb Sounder 183 GHz $H_2O$ Measurements," *J. Geophys. Res.*, **101**, 10129 (1996).
7. E. W. Chiou, M. P. McCormick, and W. P. Chu, "Upper Tropospheric Integrated Water Vapor Distributions Derived from SAGE II Observations," *EOS Transactions,* AGU, **73**, 14, (1992).
8. H. C. Pumphrey, D. Rind, J. M. Russell III, and J. E. Harries, "A Preliminary Zonal Mean Climatology of Water Vapour in the Stratosphere and Mesosphere," *Adv. Space Res.*, **21**, 1417 (1998).
9. G. M. Keating , J. S. Chiou, and N. C. Hsu, "Improved ozone reference models for the COSPAR International Reference Atmosphere," *Adv. Space Res.*, **18**, 11 (1996).
10. http://lasp.colorado.edu/snoe/
11. G. P. Anderson, J. H. Chetwynd, S. A. Clough, E. P. Shettle and F. X. Kneizys, "AFGL Atmospheric Constituent Profiles (0-120 km)," AFGL-TR-86-0110, Environmental Research Papers No. 954 (1986), ADA175173.
12. R. Rodrigo, M. J. Lopez-Gonzalez, and J. J. Lopez-Moreno, "Variability of the Neutral Mesospheric and Lower Thermospheric Composition in the Diurnal Cycle," *Planet. Space Sci.*, **39**, 803 (1991).
13. H. Trinks and K. H. Fricke, Carbon Dioxide Concentrations in the Lower Thermosphere," *J. Geophys. Res.*, **83**, 3883 (1978).
14. D. Offermann, V. Friedrich, P. Ross, and U. von Zahn, "Neutral Gas Composition Measurements Between 80 and 120 km," *Planet. Space Sci.*, **29**, 747 (1981).

15. R. D. Sharma and P. P. Wintersteiner, "Role of Carbon Dioxide in Cooling Planetary Atmospheres," *Geophys. Res. Lett.*, **17**, 2201 (1990).

16. M. Lopez-Puertas and F. W. Taylor, "Carbon Dioxide 4-3-$\mu$m Emission in the Earth's Atmosphere: A Comparison Between Numbus 7 SAMS Measurements and Non-Local Thermodynamic Between Equilibrium Radiative Transfer Calculations," *J. Geophys. Res.*, **94**, 13045 (1989).

17. C. P. Rinsland, M. R. Gunson, R. Zander, and M. Lopez-Puertas, "Middle and Upper Atmosphere Pressure-Temperature Profiles and the Abundances of $CO_2$ and CO in the Upper Atmosphere From ATMOS/Spacelab 3 Observations," *J. Geophys. Res.*, **97**, 20479 (1992).

18. D. R. Smith, P. De, S. Adler-Golden, and C. Roth, "Empirical Correlations in Thermospheric NO Density Measured From Rockets and Satellites, *J. Geophys. Res.*, **98**, 9453 (1993).

19. D. W. Rusch, J.-C. Gerard, and C. G. Fesen, "Diurnal Variation of NO, N($^2$D), and Ions in the Thermosphere: A Comparison of Satellite Measurements to a Model," *J. Geophys. Res.*, **96**, 11331 (1991).

20. C. A. Barth, "Reference Models for Thermospheric NO," *Adv. Space Res.*, **10**, 103 (1990).

21. http://www.wdc.rl.ac.uk/Help/Ap.html

22. D. Offermann, V. Friedrich, P. Ross, and U. von Zahn, "Neutral Gas Composition Measurements Between 80 and 120 km," *Planet. Space Sci*, **29**, 747, (1981).

23. W. E. Sharp, "The Measurement of Atomic Oxygen in the Mesophere and Lower Thermosphere," *Planet. Space Sci.*, **39**, 617, (1991).

24. D. F. Strobel, M. E. Summers, R. M. Bevilacqua, M. T. DeLand, M. Allen, "Vertical Constituent Transport in the Mesosphere," *J. Geophys. Res.*, **92** 6691, (1987).

25. R. R. Garcia and S. Solomon, "A Numerical Model of the Zonally Averaged Dynamical and Chemical Structure of the Middle Atmosphere," *J. Geophys. Res.*, **88**, 1379, (1983).

26. J. Bishop, "Thermospheric atomic densities and fluxes from dayside Lyman $\alpha$ measurements," *J. of Atmospheric and Solar-Terrestrial Physics*, **63**, 331, (2001).

27. W. E. Sharp and D. Kita, "In Situ Measurements of Atomic Hydrogen in the Upper Mesosphere," *J. Geophys. Res.*, **92**, 4319, (1987).

28. M. Allen, J. I. Lunine, and Y. L. Yung, "The Vertical Distribution of Ozone in the Mesophere and Lower Thermosphere," *J. Geophys. Res.*, **89**, 4841, (1984).

29. J. I. Steinfeld, S. M. Adler-Golden, and J. W. Gallagher, "Critical Survey of Data on the Spectroscopy and Kinetics of Ozone in the Mesosphere and Thermosphere," *J. Phys. Chem. Ref. Data*, **16**, 911 (1987).

30. H. Hippler, R. Rahn, and J. Troe, "Temperature and Pressure Dependence of Ozone Formation Rates in the Range 1-1000 Bar and 90-370 K," *J. Chem. Phys.*, **93**, 6560 (1990).

31. S. M. Adler-Golden, J. Vail, D. Smith, L. Jeong, and R. Sharma, "Initial Survey of Model-Data Comparisons for the CIRRIS 1A Experiment", Phillips Laboratory, Hanscom Air Force Base, SSI-TR-241, March 8, (1994).

32. R. J. Thomas, "Atomic Hydrogen and Atomic Oxygen Density in the Mesopause Region: Global and Seasonal Variations Deducted from Solar Mesosphere Explorer Near-Infrared Emissions," *J. Geophys. Res.*, **95**, 16457 (1990).

33. W. E. Sharp and D. Kita, "In situ Measurement of Atomic Hydrogen in the Upper Mesosphere, *J. Geophys. Res.*, **92**, 4319 (1987).

34. S. M. Adler-Golden, J. Gruninger, and D. R. Smith, "Derivation of Atmospheric Atomic Oxygen and Hydrogen Profiles From Ozone $\nu_3$ Band Emission," *J. Geophys. Res.*, **97**, 19509 (1992).

35. D. Offermann, V. Friedrich, P. Ross, and U. von Zahn, "Neutral Gas Composition Measurements Between 80 and 120 km," *Planet. Space Sci*, **29**, 747, (1981).

36. W. E. Sharp, The Measurement of Atomic Oxygen in the Mesophere and Lower Thermosphere, *Planet. Space Sci.*, **39**, 617, (1991).

37. D. F. Strobel, M. E. Summers, R. M. Bevilacqua, M. T. DeLand, M. Allen, "Vertical Constituent Transport in the Mesosphere," *J. Geophys. Res.*, **92** 6691, (1987).

38. R. R. Garcia and S. Solomon, "A Numerical Model of the Zonally Averaged Dynamical and Chemical Structure of the Middle Atmosphere," *J. Geophys. Res.*, **88**, 1379, (1983).

39. J. Bishop, "Thermospheric atomic densities and fluxes from dayside Lyman $\alpha$ measurements," *J. of Atmospheric and Solar-Terrestrial Physics*, **63**, 331, (2001).

40. W. E. Sharp and D. Kita, "In Situ Measurements of Atomic Hydrogen in the Upper Mesosphere," *J. Geophys. Res.*, **92**, 4319, (1987).

41. M. Allen, J. I. Lunine, and Y. L. Yung, "The Vertical Distribution of Ozone in the Mesophere and Lower Thermosphere," *J. Geophys. Res.*, **89**, 4841, (1984).

42. D. D. Grantham, I. I. Gringorten, and A. J. Kantor, Chapter 16.1 in *Handbook of Geophysics and the Space Environment*, A. S. Jursa, ed., Geophys. Lab., Hanscom AFB, MA (1985), ADA167000.

43. R. Rodrigo, J. J. Lopez-Moreno, M. Lopez-Puertas, F. Moreno, and A. Morlina, "Neutral Atmospheric Composition Between 60 and 200 km; A Theoretical Model for Mid-Latitudes", *Planet. Space Sci.*, **34**, 723, (1986)

44. R. J. Thomas and R. A. Young, "Measurement of Atomic Oxygen and Related Airglows in the Lower Thermosphere", *J. Geophys. Res.*, **86**, 7389, (1981)

45. J. G. Anderson, "The Absolute Concentration of $O(^3P)$ in the Earth's Stratosphere", *Geophys, Res. Lett.*, **3**, 231, (1975)

46. T. J. Keneshea, P. Zimmerman, and C. R. Philbrick, "A Dynamic Model of the Mesosphere and Lower Thermosphere", *Planet. Space Sci.*, **27**, 385, (1979)

47. E. J. Llewellyn and G. Witt, *Planet. Space Sci.*, "The Measurment of Ozone Concentrations at High Latitude During the Twilight", **25**, 165, (1977)

48. E. Battaner and R. Rodrigo, *Planet. Space Sci.*, **29**, (1981)

49. D. E. Miller and P. Ryder, *Planet. Space Sci.*, **21**, 963, (1973)

50. L. H. Weeks, W. J. Wilson, J. S. Randhawa, and H. Trinks, *J. Geophys. Res.*, **83**, 978, (1978)

51. A. J. Krueger and R. A. Minzner, "A Mid-Latitude Ozone Model for the 1976 U.S. Standard Atmosphere", *J. Geophys. Res.*, **81**, 4477, (1976)

52. P. B. Hays and J. J. Olivero, *Planet. Space Sci.*, **18**, 1729, (1970)

53. J. W. Waters, W. J. Wilson, and F. I. Shimabukuro, *Science*, **191**, 1174, (1976)

54. M. Ackerman, *J. Atmos. Terr. Phys.*, **41**, 723, (1979)

55. R. T. Clancy, D. O. Muhleman, and M. Allen, *J. Geophys. Res.*, **89**, 9673, (1984)

56. T. C. James and J. B. Kumer, *J. Geophys. Res.*, **78**, 8320, (1973)

57. A. Girard, J. Besson, D. Brard, J. Laurent, M. P. Lemaitre, C. Lippens, C. Muller, J. Vercheval, and M. Ackerman, "Global Results of Grille Spectrometer Experiment on Board *Spacelab* I", *Planet. Space Sci.*, **36**, 291, (1988)

58. S. Adler-Golden, P. De, D. Smith, and A. D'Agati, "Mesospheric Water Vapor Sounding Using Earth-Limb Pure-Rotational Emission in the LWIR", *Geo. Res. Lett.*, **20**, 1551, (1993)

59. W. Swider and R. S. Narcisi, *J. Geophys. Res.*, **80**, 655, (1975)

60. H. E. Radford, M. M. Litvak, C. A. Gottlieb, E. W. Gottlieb, S. K. Rosenthal, and A. E. Lilley, *J. Geophys. Res.*, **82**, 472, (1977)

61. C. J. Gibbins, P. R. Schwartz, D. L. Thacker, and R. M. Bevilacqua, *Geophys, Res. Lett.*, **9**, 131, (1982)

62. S. Solomon, E. E. Ferguson, D. W. Fahey, and P. J. Crutzen, *Planet. Space Sci.*, **30**, 1117, (1982)

63. World Meteorological Organization, "The Stratosphere 1981: Theory and measurements", *WMO Global Ozone Res. And Monit. Proj. Rep. 11*, Geneva, Switzerland, 1982

# APPENDIX A: SUMMARY OF CHANGES

## A.1 Summary of Changes from SAG 0.92 to SAG 2.0

The SAG 2.0 program now:

- Includes the patched MSISE90 database release, which corrects an error in SUBROUTINE GHP6 when using METER6(.TRUE.). This error does not affect SAG output but was corrected to aid future code development.
- Includes the NRLMSISE-00 database.
- Offers a choice of
  - using either MSISE-90 or NRLMSISE-00 database.
  - including SNOE database for NO density.
  - including URAP $H_2O$ database.
  - using revised O atom profiles.
  - using revised H atom profiles.
  - using either Geodetic or Geocentric Latitude input.
- Is a FORTRAN SUBROUTINE.
- Generates a default set of altitudes if an altitude file is not found.
- Executes when the input parameter file is not found.
- Includes a quality assurance routine to test SAG installations.
- Includes a new atmosphere output file format for the file ATMOUT.DAT.
- Has a centralized error handling routine.

## APPENDIX B: PROGRAM AND I/O STRUCTURE

### B.1 Main Program

The main subroutine, named SAG, serves to call two subroutines, the menu subroutine for gathering input information and the atmosphere generator subroutine which uses this information. These are described below.

### B.2 Menu Subroutine

The menu subroutine, named SETDRI, gathers information on the day of the year, universal time or local solar time, latitude, longitude, F10.7 daily solar flux for previous day and F10.7A monthly average solar flux, daily Ap, the atmosphere file name, and the comment line appearing in the atmosphere file. At the beginning of execution, information from the last run is entered from file "drivstor.dat". At the end of execution, the "drivstor.dat" data are updated.

### B.3 Atmosphere Generator Subroutine

The atmosphere generator subroutine, named DRI, creates the atmosphere file. Input files opened are the appropriate "drivht" file, which contains the altitude list and the SHARC/SAMM switch, and the NRL database[3] files (see below). DRI calls on the MSISE-90/NRLMSISE-00 subroutine GTD6/GTD7.

In addition to creating the SHARC/SAMM atmosphere file, the delivered version of DRI may also create additional output files that are useful for research purposes (see Section B.5).

### B.4 List of Input Files

4 input files: drivstor.dat (updated by SAG), drivht.mod, drivht.sam, drivht.sha

10 NRL data files in subdirectory NRLDAT: CH4.NRL, CO.NRL, H2O.NRL, HNO3.NRL, N2O.NRL, NO2.NRL, O3D.NRL, O3R.NRL, OAT.NRL, TEMP.NRL.

1 URAP data file in subdirectory UARSDAT: H2O.DAT

1 SNOE data file in subdirectory SNOE: SNOE.DAT

Total files = 16.

### B.5 Output Files

An example of an atmosphere output file (which has a user-specified name) is given in Appendix C. The SHARC atmosphere files are identical to the SAMM atmosphere files except for the omission of the species $N_2O$, $HNO_3$, $NO_2$, $SO_2$, and $NH_3$.

The delivered code may also create one or more optional output files useful for research purposes. These are:

(1) "tape5.dat", an atmosphere file in the MODTRAN input format. This file is written only if the MODTRAN or SAMM species ($H_2O$,$CO_2$,$O_3$,$N_2O$,CO,$CH_4$,$O_2$,NO,$SO_2$,$NO_2$,$NH_3$,$HNO_3$) are requested;

(2) "norad.dat", a file containing an altitude profile of the approximate NO 5.3 μm volumetric emission, valid above 100 km;

(3) "dumpfil.dat", a file containing a number of outputs including pressures, temperatures, number densities, concentrations, and altitudes listed in columns. Additional values from the NRL database[3] (temperature and high-altitude ozone), which are not used in the output atmosphere are provided for comparison purposes. "dumpfil.dat" differs from the other output files in that each time the "Generate atmosphere" command is given within the SAG session the "dumpfil.dat" output is appended rather than overwritten.

(4) "ATMOUT.DAT", a file of the calculated atmosphere in an easily readable format.

(5) "QAERROR.log", a file generated if a QA Test fails, which shows the failed comparison.

\

# APPENDIX C: SAMPLE INPUTS AND OUTPUTS

## C.1 Sample Interactive Session

This section features an illustrative interactive session with SAG in which an atmosphere is generated for SAMM. The user responses are contained in braces, { }.

In this session, a default value was entered for the solar flux (moderate) and the local time was specified as 10 AM. The day of the year remained as day 135. Note that after the local time was changed, updated values for the solar angle and the universal time appeared in the Parameter Menu listing.

SHARC/SAMM ATMOSPHERE GENERATOR
Version 2.0

MAIN MENU

1 Change header line comment (64 chars max) from
HIGH LATITUDE - WINTER
2 Change output file name. Current name is
SAGTEST.ATM
3 Change or inspect parameter values
4 Enter defaults
5 Generate atmosphere
6 Run QA Tests
7 Quit

Enter item no:
{4}

DEFAULT MENU

Current defaults are

1 Day (d) or night (n):
2 Equatorial (e), mid (m) or high (h) latitude:
3 NH Winter (w), spring (p), summer (s) or fall (f):
4 Low (l), medium (m) or high (h) solar flux: m
5 Low (l), medium (m) or high (h) geomagnetic activity: m
6 SHARC (s) SAMM (a) MODTRAN (m) or custom (c) altitudes: a

Enter [n,letter] or [0,0] to return to main menu:
{2,m}

Enter [n,letter] or [0,0] to return to main menu:
{0}

1 Day (d) or night (n):
2 Equatorial (e), mid (m) or high (h) latitude: m
3 NH Winter (w), spring (p), summer (s) or fall (f):
4 Low (l), medium (m) or high (h) solar flux: m
5 Low (l), medium (m) or high (h) geomagnetic activity: m
6 SHARC (s) SAMM (a) MODTRAN (m) or custom (c) altitudes: a

MAIN MENU

1 Change header line comment (64 chars max) from
HIGH LATITUDE - WINTER
2 Change output file name. Current name is
SAGTEST.ATM
3 Change or inspect parameter values
4 Enter defaults
5 Generate atmosphere
6 Run QA Tests
7 Quit

```
  Enter item no:
{3}

PARAMETER MENU

  Current parameters are

1 Daily Ap =  15.0
2 F10.7 (81 day centered average of F10.7) =  120.0
3 F10.7A =  120.0
4 Latitude Type =  1  Latitude (- =S) =  35.2
  Latitude Type: Geocentric(0), Geodetic(1)
5 Longitude =  30.0
6 UT (sec) = 79200.
7 Solar Time (hrs) =  0.00
8 Month =  5
9 Day =  15
10 Year = 2002
11 Day Number =  135
12 Solar Zenith = 125.82
13 H, O, URAP, SNOE, NRLMSISE-00 =  T T T T T

  Enter item number [n] or [0] to return to main menu:
{7}
item= 7
  Enter new [value]:
{10}
Solar Zenith Angle = 64.98
  Enter item number [n] or [0] to return to main menu:
{0}
item= 0

1 Daily Ap =  15.0
2 F10.7 (81 day centered average of F10.7) =  120.0
3 F10.7A =  120.0
4 Latitude Type =  1  Latitude (- =S) =  35.2
  Latitude Type: Geocentric(0), Geodetic(1)
5 Longitude =  30.0
6 UT (sec) = 28800.
7 Solar Time (hrs) =  10.00
8 Month =  5
9 Day =  15
10 Year = 2002
11 Day Number =  135
12 Solar Zenith =  30.45
13 H, O, URAP, SNOE, NRLMSISE-00 =  T T T T T

MAIN MENU

1 Change header line comment (64 chars max) from
HIGH LATITUDE - WINTER
2 Change output file name.  Current name is
SAGTEST.ATM
3 Change or inspect parameter values
4 Enter defaults
5 Generate atmosphere
```

```
6 Run QA Tests
7 Quit

  Enter item no:
{5}
 sunrise LST, sunset LST=    7.140   16.860

 SHARC/SAMM ATMOSPHERE GENERATOR
       Version 2.0

 MAIN MENU

1 Change header line comment (64 chars max) from
 HIGH LATITUDE - WINTER
2 Change output file name.  Current name is
 SAGTEST.ATM
3 Change or inspect parameter values
4 Enter defaults
5 Generate atmosphere
6 Run QA Tests
7 Quit

  Enter item no:
{7}
```

## C.2 Atmosphere Output File (for SAMM) from the Interactive Session

```
ATMOSPHERE NAME HIGH LATITUDE - WINTER
SAGTEST.ATM
END
NUMBER OF LAYERS
103
END
DAY-NIGHT VARIABLE AND EXOATMOSPHERIC TEMPERATURE
 DAY   1017.81
END
SPECIES
O2 O CO2 N2 NO O3 H OH CO H2O CH4 HNO3 N2O NH3 NO2 SO2
END
ALTITUDES
  0.00  1.00  2.00  3.00  4.00
  5.00  6.00  7.00  8.00  9.00
 10.00 11.00 12.00 13.00 14.00
 15.00 16.00 17.00 18.00 19.00
 20.00 21.00 22.00 23.00 24.00
 26.00 28.00 30.00 32.00 34.00
 36.00 38.00 40.00 42.00 44.00
 46.00 48.00 50.00 52.00 54.00
 56.00 58.00 60.00 62.00 64.00
 66.00 68.00 70.00 72.00 74.00
 76.00 78.00 80.00 82.00 84.00
 86.00 88.00 90.00 92.00 94.00
 96.00 98.00 100.00 102.00 104.00
106.00 108.00 110.00 112.00 114.00
116.00 118.00 120.00 122.00 124.00
126.00 128.00 130.00 132.00 134.00
```

136.00 138.00 140.00 142.00 144.00
146.00 148.00 150.00 160.00 170.00
180.00 190.00 200.00 210.00 220.00
230.00 240.00 250.00 260.00 270.00
280.00 290.00 300.00
END
TEMPERATURES
0.2932E+03 0.2890E+03 0.2837E+03 0.2776E+03 0.2709E+03
0.2639E+03 0.2568E+03 0.2497E+03 0.2427E+03 0.2361E+03
0.2299E+03 0.2241E+03 0.2189E+03 0.2146E+03 0.2113E+03
0.2091E+03 0.2081E+03 0.2081E+03 0.2089E+03 0.2102E+03
0.2118E+03 0.2134E+03 0.2151E+03 0.2169E+03 0.2187E+03
0.2226E+03 0.2267E+03 0.2312E+03 0.2361E+03 0.2417E+03
0.2481E+03 0.2550E+03 0.2617E+03 0.2675E+03 0.2716E+03
0.2732E+03 0.2720E+03 0.2688E+03 0.2640E+03 0.2584E+03
0.2525E+03 0.2467E+03 0.2408E+03 0.2351E+03 0.2296E+03
0.2241E+03 0.2189E+03 0.2138E+03 0.2090E+03 0.2040E+03
0.1983E+03 0.1923E+03 0.1865E+03 0.1813E+03 0.1770E+03
0.1738E+03 0.1718E+03 0.1714E+03 0.1727E+03 0.1757E+03
0.1806E+03 0.1874E+03 0.1965E+03 0.2079E+03 0.2219E+03
0.2381E+03 0.2562E+03 0.2750E+03 0.2934E+03 0.3110E+03
0.3284E+03 0.3462E+03 0.3658E+03 0.3889E+03 0.4179E+03
0.4478E+03 0.4762E+03 0.5031E+03 0.5287E+03 0.5530E+03
0.5761E+03 0.5980E+03 0.6189E+03 0.6387E+03 0.6574E+03
0.6753E+03 0.6923E+03 0.7084E+03 0.7776E+03 0.8312E+03
0.8727E+03 0.9049E+03 0.9299E+03 0.9493E+03 0.9644E+03
0.9761E+03 0.9852E+03 0.9923E+03 0.9979E+03 0.1002E+04
0.1006E+04 0.1008E+04 0.1010E+04
END
N2 DENSITIES
0.1977E+20 0.1784E+20 0.1613E+20 0.1460E+20 0.1321E+20
0.1194E+20 0.1077E+20 0.9682E+19 0.8672E+19 0.7734E+19
0.6865E+19 0.6062E+19 0.5322E+19 0.4641E+19 0.4018E+19
0.3455E+19 0.2950E+19 0.2505E+19 0.2121E+19 0.1793E+19
0.1515E+19 0.1282E+19 0.1086E+19 0.9206E+18 0.7815E+18
0.5650E+18 0.4104E+18 0.2995E+18 0.2196E+18 0.1617E+18
0.1196E+18 0.8898E+17 0.6680E+17 0.5066E+17 0.3888E+17
0.3020E+17 0.2370E+17 0.1872E+17 0.1481E+17 0.1170E+17
0.9209E+16 0.7208E+16 0.5608E+16 0.4336E+16 0.3331E+16
0.2541E+16 0.1924E+16 0.1447E+16 0.1080E+16 0.8002E+15
0.5914E+15 0.4337E+15 0.3148E+15 0.2257E+15 0.1597E+15
0.1116E+15 0.7704E+14 0.5263E+14 0.3567E+14 0.2408E+14
0.1625E+14 0.1101E+14 0.7496E+13 0.5146E+13 0.3574E+13
0.2518E+13 0.1806E+13 0.1322E+13 0.9895E+12 0.7556E+12
0.5862E+12 0.4602E+12 0.3642E+12 0.2893E+12 0.2300E+12
0.1853E+12 0.1519E+12 0.1263E+12 0.1063E+12 0.9038E+11
0.7756E+11 0.6708E+11 0.5843E+11 0.5121E+11 0.4513E+11
0.3997E+11 0.3555E+11 0.3175E+11 0.1896E+11 0.1201E+11
0.7931E+10 0.5388E+10 0.3738E+10 0.2634E+10 0.1878E+10
0.1351E+10 0.9791E+09 0.7134E+09 0.5222E+09 0.3837E+09
0.2827E+09 0.2089E+09 0.1546E+09
END
O2 DENSITIES
0.5303E+19 0.4785E+19 0.4328E+19 0.3917E+19 0.3545E+19
0.3204E+19 0.2889E+19 0.2597E+19 0.2326E+19 0.2075E+19
0.1842E+19 0.1626E+19 0.1428E+19 0.1245E+19 0.1078E+19

0.9268E+18 0.7913E+18 0.6721E+18 0.5690E+18 0.4810E+18
0.4065E+18 0.3439E+18 0.2913E+18 0.2470E+18 0.2096E+18
0.1516E+18 0.1101E+18 0.8036E+17 0.5892E+17 0.4338E+17
0.3208E+17 0.2387E+17 0.1792E+17 0.1359E+17 0.1043E+17
0.8102E+16 0.6359E+16 0.5021E+16 0.3973E+16 0.3139E+16
0.2471E+16 0.1934E+16 0.1505E+16 0.1163E+16 0.8908E+15
0.6768E+15 0.5106E+15 0.3823E+15 0.2842E+15 0.2098E+15
0.1544E+15 0.1127E+15 0.8128E+14 0.5786E+14 0.4058E+14
0.2805E+14 0.1911E+14 0.1284E+14 0.8534E+13 0.5627E+13
0.3693E+13 0.2421E+13 0.1588E+13 0.1046E+13 0.6943E+12
0.4660E+12 0.3174E+12 0.2202E+12 0.1560E+12 0.1126E+12
0.8252E+11 0.6116E+11 0.4570E+11 0.3431E+11 0.2581E+11
0.1973E+11 0.1538E+11 0.1218E+11 0.9799E+10 0.7985E+10
0.6584E+10 0.5487E+10 0.4616E+10 0.3918E+10 0.3351E+10
0.2887E+10 0.2503E+10 0.2183E+10 0.1182E+10 0.6960E+09
0.4322E+09 0.2781E+09 0.1834E+09 0.1231E+09 0.8377E+08
0.5758E+08 0.3988E+08 0.2780E+08 0.1948E+08 0.1370E+08
0.9667E+07 0.6842E+07 0.4854E+07
END
O DENSITIES
0.1308E+03 0.2443E+03 0.4509E+03 0.8229E+03 0.1484E+04
0.2648E+04 0.4668E+04 0.8137E+04 0.1402E+05 0.2389E+05
0.4023E+05 0.6699E+05 0.1103E+06 0.1794E+06 0.2887E+06
0.4591E+06 0.7219E+06 0.1122E+07 0.1724E+07 0.2620E+07
0.3934E+07 0.5841E+07 0.8574E+07 0.1244E+08 0.1785E+08
0.3550E+08 0.6743E+08 0.1223E+09 0.2120E+09 0.3510E+09
0.5551E+09 0.8385E+09 0.1210E+10 0.1667E+10 0.2195E+10
0.2760E+10 0.3316E+10 0.3804E+10 0.4170E+10 0.4365E+10
0.4380E+10 0.4296E+10 0.4135E+10 0.3903E+10 0.3615E+10
0.3284E+10 0.2927E+10 0.2559E+10 0.2195E+10 0.1870E+10
0.1662E+10 0.1949E+10 0.4052E+10 0.1144E+11 0.3030E+11
0.6706E+11 0.1226E+12 0.1881E+12 0.2484E+12 0.2900E+12
0.3072E+12 0.3026E+12 0.2825E+12 0.2540E+12 0.2231E+12
0.1935E+12 0.1671E+12 0.1448E+12 0.1266E+12 0.1118E+12
0.9938E+11 0.8883E+11 0.7957E+11 0.7118E+11 0.6086E+11
0.5243E+11 0.4570E+11 0.4024E+11 0.3573E+11 0.3197E+11
0.2879E+11 0.2607E+11 0.2373E+11 0.2170E+11 0.1993E+11
0.1837E+11 0.1699E+11 0.1576E+11 0.1124E+11 0.8398E+10
0.6476E+10 0.5106E+10 0.4091E+10 0.3318E+10 0.2715E+10
0.2237E+10 0.1853E+10 0.1542E+10 0.1287E+10 0.1077E+10
0.9029E+09 0.7586E+09 0.6383E+09
END
CO2 DENSITIES
0.8607E+16 0.7767E+16 0.7024E+16 0.6358E+16 0.5754E+16
0.5200E+16 0.4689E+16 0.4216E+16 0.3776E+16 0.3368E+16
0.2989E+16 0.2640E+16 0.2317E+16 0.2021E+16 0.1750E+16
0.1504E+16 0.1284E+16 0.1091E+16 0.9236E+15 0.7807E+15
0.6598E+15 0.5582E+15 0.4728E+15 0.4008E+15 0.3403E+15
0.2460E+15 0.1787E+15 0.1304E+15 0.9563E+14 0.7042E+14
0.5206E+14 0.3875E+14 0.2908E+14 0.2206E+14 0.1693E+14
0.1315E+14 0.1032E+14 0.8149E+13 0.6448E+13 0.5095E+13
0.4010E+13 0.3139E+13 0.2442E+13 0.1888E+13 0.1450E+13
0.1105E+13 0.8369E+12 0.6290E+12 0.4692E+12 0.3475E+12
0.2565E+12 0.1879E+12 0.1361E+12 0.9730E+11 0.6858E+11
0.4763E+11 0.3261E+11 0.2201E+11 0.1384E+11 0.8614E+10
0.5324E+10 0.3274E+10 0.2007E+10 0.1229E+10 0.7551E+09

0.4674E+09 0.2930E+09 0.1869E+09 0.1218E+09 0.8095E+08
0.5466E+08 0.3737E+08 0.2577E+08 0.1874E+08 0.1365E+08
0.1012E+08 0.7667E+07 0.5914E+07 0.4634E+07 0.3681E+07
0.2959E+07 0.2403E+07 0.1970E+07 0.1628E+07 0.1356E+07
0.1136E+07 0.9580E+06 0.8119E+06 0.3829E+06 0.1953E+06
0.1050E+06 0.5864E+05 0.3365E+05 0.1971E+05 0.1172E+05
0.7054E+04 0.4286E+04 0.2624E+04 0.1616E+04 0.9999E+03
0.6212E+03 0.3873E+03 0.2422E+03
END
H DENSITIES
0.1000E-04 0.1000E-04 0.1000E-04 0.1000E-04 0.1000E-04
0.1000E-04 0.1000E-04 0.1000E-04 0.1000E-04 0.1000E-04
0.1000E-04 0.1000E-04 0.1000E-04 0.1000E-04 0.1000E-04
0.1000E-04 0.1000E-04 0.1000E-04 0.1000E-04 0.2330E-04
0.5697E-04 0.1374E-03 0.3268E-03 0.7665E-03 0.1773E-02
0.9103E-02 0.4421E-01 0.2031E+00 0.8830E+00 0.3631E+01
0.1413E+02 0.5200E+02 0.1811E+03 0.5966E+03 0.1859E+04
0.5482E+04 0.1529E+05 0.4036E+05 0.1008E+06 0.2380E+06
0.5318E+06 0.1124E+07 0.2249E+07 0.4254E+07 0.7616E+07
0.1290E+08 0.2066E+08 0.3132E+08 0.4491E+08 0.6093E+08
0.7819E+08 0.9494E+08 0.1091E+09 0.1185E+09 0.1260E+09
0.1132E+09 0.8872E+08 0.6665E+08 0.4991E+08 0.3794E+08
0.2950E+08 0.2353E+08 0.1922E+08 0.1605E+08 0.1361E+08
0.1166E+08 0.1005E+08 0.8672E+07 0.7457E+07 0.6387E+07
0.5449E+07 0.4633E+07 0.3935E+07 0.3348E+07 0.2871E+07
0.2481E+07 0.2157E+07 0.1886E+07 0.1657E+07 0.1463E+07
0.1297E+07 0.1156E+07 0.1034E+07 0.9284E+06 0.8375E+06
0.7588E+06 0.6904E+06 0.6309E+06 0.4279E+06 0.3197E+06
0.2588E+06 0.2228E+06 0.2006E+06 0.1863E+06 0.1766E+06
0.1699E+06 0.1649E+06 0.1610E+06 0.1578E+06 0.1551E+06
0.1527E+06 0.1505E+06 0.1485E+06
END
NO DENSITIES
0.7592E+10 0.6851E+10 0.6196E+10 0.5608E+10 0.5075E+10
0.4587E+10 0.4136E+10 0.3718E+10 0.3331E+10 0.2970E+10
0.2637E+10 0.2328E+10 0.2044E+10 0.1776E+10 0.1518E+10
0.1252E+10 0.1012E+10 0.8083E+09 0.6517E+09 0.5601E+09
0.4947E+09 0.4546E+09 0.4267E+09 0.4243E+09 0.4512E+09
0.6363E+09 0.7659E+09 0.9395E+09 0.1126E+10 0.1232E+10
0.1217E+10 0.1103E+10 0.9578E+09 0.7625E+09 0.5863E+09
0.4414E+09 0.3294E+09 0.2468E+09 0.1937E+09 0.1519E+09
0.1191E+09 0.9320E+08 0.7252E+08 0.5651E+08 0.4372E+08
0.3420E+08 0.2705E+08 0.2123E+08 0.1812E+08 0.1535E+08
0.1342E+08 0.1206E+08 0.1072E+08 0.1211E+08 0.1368E+08
0.1545E+08 0.1746E+08 0.1972E+08 0.2228E+08 0.2518E+08
0.2844E+08 0.3213E+08 0.3630E+08 0.8448E+08 0.1052E+09
0.1237E+09 0.1352E+09 0.1370E+09 0.1297E+09 0.1165E+09
0.1012E+09 0.8664E+08 0.7404E+08 0.6368E+08 0.5573E+08
0.4999E+08 0.4592E+08 0.4292E+08 0.3446E+08 0.2902E+08
0.2471E+08 0.2097E+08 0.1780E+08 0.1525E+08 0.1307E+08
0.1116E+08 0.9535E+07 0.8178E+07 0.5601E+07 0.3834E+07
0.2622E+07 0.1781E+07 0.1210E+07 0.8204E+06 0.5560E+06
0.3763E+06 0.2545E+06 0.1718E+06 0.1159E+06 0.7806E+05
0.5250E+05 0.3525E+05 0.2362E+05
END
O3 DENSITIES

0.1003E+13 0.1066E+13 0.1137E+13 0.1063E+13 0.9942E+12
0.9314E+12 0.8707E+12 0.8371E+12 0.8018E+12 0.8730E+12
0.9460E+12 0.1139E+13 0.1364E+13 0.1628E+13 0.1929E+13
0.2256E+13 0.2621E+13 0.2854E+13 0.3098E+13 0.3356E+13
0.3635E+13 0.3942E+13 0.4281E+13 0.4654E+13 0.5065E+13
0.4284E+13 0.3577E+13 0.3001E+13 0.2269E+13 0.1723E+13
0.1246E+13 0.8597E+12 0.5985E+12 0.3776E+12 0.2410E+12
0.1555E+12 0.1012E+12 0.6630E+11 0.4477E+11 0.3019E+11
0.1990E+11 0.1280E+11 0.8189E+10 0.4993E+10 0.3023E+10
0.1775E+10 0.1011E+10 0.5720E+09 0.3716E+09 0.2397E+09
0.1712E+09 0.1123E+09 0.5757E+08 0.6015E+08 0.6463E+08
0.6495E+08 0.5959E+08 0.4366E+08 0.2634E+08 0.1364E+08
0.6333E+07 0.2752E+07 0.1164E+07 0.4976E+06 0.2224E+06
0.1059E+06 0.5394E+05 0.2928E+05 0.1686E+05 0.1015E+05
0.6307E+04 0.4000E+04 0.2559E+04 0.1629E+04 0.9892E+03
0.6164E+03 0.3999E+03 0.2687E+03 0.1862E+03 0.1325E+03
0.9665E+02 0.7199E+02 0.5463E+02 0.4216E+02 0.3302E+02
0.2621E+02 0.2105E+02 0.1709E+02 0.6823E+01 0.3148E+01
0.1587E+01 0.8471E+00 0.4695E+00 0.2669E+00 0.1545E+00
0.9053E-01 0.5353E-01 0.3186E-01 0.1906E-01 0.1144E-01
0.6884E-02 0.4152E-02 0.2509E-02
END
OH DENSITIES
0.1113E+07 0.1005E+07 0.9087E+06 0.8225E+06 0.7443E+06
0.6727E+06 0.6066E+06 0.5466E+06 0.4940E+06 0.4515E+06
0.4113E+06 0.3725E+06 0.3366E+06 0.3083E+06 0.2907E+06
0.2985E+06 0.3115E+06 0.3336E+06 0.3530E+06 0.3765E+06
0.4190E+06 0.5580E+06 0.7075E+06 0.8945E+06 0.1161E+07
0.2198E+07 0.3114E+07 0.4487E+07 0.7723E+07 0.1207E+08
0.1699E+08 0.2147E+08 0.2437E+08 0.2453E+08 0.2320E+08
0.2077E+08 0.1812E+08 0.1617E+08 0.1469E+08 0.1333E+08
0.1270E+08 0.1271E+08 0.1264E+08 0.1321E+08 0.1371E+08
0.1384E+08 0.1361E+08 0.1328E+08 0.1182E+08 0.6944E+07
0.4080E+07 0.2397E+07 0.1408E+07 0.5358E+06 0.2200E+06
0.8637E+05 0.3317E+05 0.1183E+05 0.4115E+04 0.1439E+04
0.5187E+03 0.1963E+03 0.7944E+02 0.3490E+02 0.1681E+02
0.8847E+01 0.5006E+01 0.2981E+01 0.1833E+01 0.1149E+01
0.7285E+00 0.4654E+00 0.2985E+00 0.1918E+00 0.1246E+00
0.8252E-01 0.5604E-01 0.3895E-01 0.2766E-01 0.2003E-01
0.1476E-01 0.1107E-01 0.8421E-02 0.6500E-02 0.5083E-02
0.4024E-02 0.3222E-02 0.2607E-02 0.1036E-02 0.4927E-03
0.2663E-03 0.1575E-03 0.9914E-04 0.6506E-04 0.4389E-04
0.3016E-04 0.2097E-04 0.1469E-04 0.1034E-04 0.7299E-05
0.5164E-05 0.3658E-05 0.2593E-05
END
CO DENSITIES
0.2784E+13 0.2467E+13 0.2210E+13 0.1973E+13 0.1760E+13
0.1575E+13 0.1407E+13 0.1253E+13 0.1117E+13 0.9860E+12
0.8667E+12 0.7574E+12 0.6514E+12 0.5383E+12 0.4380E+12
0.3236E+12 0.2310E+12 0.1546E+12 0.9559E+11 0.7383E+11
0.5658E+11 0.4368E+11 0.3417E+11 0.2601E+11 0.2004E+11
0.1247E+11 0.7682E+10 0.4602E+10 0.4034E+10 0.3456E+10
0.2919E+10 0.2446E+10 0.2041E+10 0.1844E+10 0.1641E+10
0.1640E+10 0.1721E+10 0.1701E+10 0.1889E+10 0.1921E+10
0.1991E+10 0.2043E+10 0.1967E+10 0.1978E+10 0.1870E+10
0.1742E+10 0.1596E+10 0.1407E+10 0.1362E+10 0.1240E+10

0.1194E+10 0.1158E+10 0.1045E+10 0.1007E+10 0.8951E+09
0.7708E+09 0.6449E+09 0.5175E+09 0.4202E+09 0.3307E+09
0.2591E+09 0.2027E+09 0.1567E+09 0.1212E+09 0.9375E+08
0.7242E+08 0.5625E+08 0.4441E+08 0.3519E+08 0.2842E+08
0.2313E+08 0.1891E+08 0.1560E+08 0.1258E+08 0.1008E+08
0.8198E+07 0.6779E+07 0.5688E+07 0.4831E+07 0.4147E+07
0.3593E+07 0.3138E+07 0.2760E+07 0.2443E+07 0.2175E+07
0.1947E+07 0.1750E+07 0.1580E+07 0.9973E+06 0.6707E+06
0.4715E+06 0.3422E+06 0.2545E+06 0.1930E+06 0.1485E+06
0.1158E+06 0.9121E+05 0.7249E+05 0.5806E+05 0.4681E+05
0.3796E+05 0.3094E+05 0.2533E+05
END
H2O DENSITIES
0.4345E+18 0.3130E+18 0.2073E+18 0.1271E+18 0.7269E+17
0.3902E+17 0.1979E+17 0.9531E+16 0.4373E+16 0.2197E+16
0.1099E+16 0.5467E+15 0.2704E+15 0.1329E+15 0.6482E+14
0.3140E+14 0.1510E+14 0.1236E+14 0.1039E+14 0.9051E+13
0.8063E+13 0.7143E+13 0.6160E+13 0.5212E+13 0.4384E+13
0.3167E+13 0.2416E+13 0.1864E+13 0.1414E+13 0.1061E+13
0.8017E+12 0.6108E+12 0.4666E+12 0.3580E+12 0.2792E+12
0.2202E+12 0.1747E+12 0.1406E+12 0.1130E+12 0.8921E+11
0.6942E+11 0.5277E+11 0.3984E+11 0.3079E+11 0.2356E+11
0.1810E+11 0.1344E+11 0.9018E+10 0.5787E+10 0.3652E+10
0.2205E+10 0.1270E+10 0.7876E+09 0.4794E+09 0.2890E+09
0.1715E+09 0.9879E+08 0.5632E+08 0.3180E+08 0.1789E+08
0.1039E+08 0.6243E+07 0.3776E+07 0.2434E+07 0.1589E+07
0.1046E+07 0.6972E+06 0.4749E+06 0.3366E+06 0.2437E+06
0.1785E+06 0.1318E+06 0.9824E+05 0.7922E+05 0.6351E+05
0.5163E+05 0.4270E+05 0.3583E+05 0.3043E+05 0.2612E+05
0.2263E+05 0.1976E+05 0.1739E+05 0.1539E+05 0.1370E+05
0.1226E+05 0.1102E+05 0.9952E+04 0.6282E+04 0.4225E+04
0.2970E+04 0.2155E+04 0.1603E+04 0.1215E+04 0.9356E+03
0.7293E+03 0.5745E+03 0.4566E+03 0.3657E+03 0.2948E+03
0.2391E+03 0.1949E+03 0.1596E+03
END
CH4 DENSITIES
0.4366E+14 0.3888E+14 0.3470E+14 0.3097E+14 0.2765E+14
0.2464E+14 0.2191E+14 0.1941E+14 0.1714E+14 0.1506E+14
0.1317E+14 0.1146E+14 0.9901E+13 0.8500E+13 0.7241E+13
0.6125E+13 0.5144E+13 0.4296E+13 0.3576E+13 0.2972E+13
0.2468E+13 0.2050E+13 0.1705E+13 0.1419E+13 0.1182E+13
0.8215E+12 0.5730E+12 0.4009E+12 0.2671E+12 0.1769E+12
0.1166E+12 0.7655E+11 0.4980E+11 0.3473E+11 0.2431E+11
0.1747E+11 0.1292E+11 0.9571E+10 0.7153E+10 0.5320E+10
0.3943E+10 0.2909E+10 0.2126E+10 0.1551E+10 0.1120E+10
0.8035E+09 0.5734E+09 0.4047E+09 0.2848E+09 0.1983E+09
0.1378E+09 0.9518E+08 0.6478E+08 0.4386E+08 0.2921E+08
0.1919E+08 0.1244E+08 0.7954E+07 0.5088E+07 0.3233E+07
0.2056E+07 0.1313E+07 0.8404E+06 0.5468E+06 0.3589E+06
0.2390E+06 0.1620E+06 0.1118E+06 0.7939E+05 0.5737E+05
0.4237E+05 0.3191E+05 0.2419E+05 0.1950E+05 0.1564E+05
0.1271E+05 0.1051E+05 0.8820E+04 0.7491E+04 0.6430E+04
0.5571E+04 0.4865E+04 0.4280E+04 0.3789E+04 0.3373E+04
0.3019E+04 0.2714E+04 0.2450E+04 0.1546E+04 0.1040E+04
0.7310E+03 0.5306E+03 0.3947E+03 0.2992E+03 0.2303E+03
0.1795E+03 0.1414E+03 0.1124E+03 0.9003E+02 0.7258E+02

0.5886E+02 0.4797E+02 0.3928E+02
END
HNO3 DENSITIES
0.1204E+11 0.1202E+11 0.1205E+11 0.1207E+11 0.1210E+11
0.1211E+11 0.1208E+11 0.1204E+11 0.1195E+11 0.1178E+11
0.1159E+11 0.1132E+11 0.1100E+11 0.1063E+11 0.1020E+11
0.9706E+10 0.9172E+10 0.8632E+10 0.8090E+10 0.7577E+10
0.7944E+10 0.8037E+10 0.7531E+10 0.6963E+10 0.5966E+10
0.3880E+10 0.2315E+10 0.1388E+10 0.7799E+09 0.4401E+09
0.2257E+09 0.1055E+09 0.4974E+08 0.2371E+08 0.1143E+08
0.5578E+07 0.2750E+07 0.1364E+07 0.6779E+06 0.3366E+06
0.1664E+06 0.8181E+05 0.3998E+05 0.1941E+05 0.9359E+04
0.4480E+04 0.2130E+04 0.1005E+04 0.4708E+03 0.2190E+03
0.1016E+03 0.4675E+02 0.2128E+02 0.9575E+01 0.4251E+01
0.1862E+01 0.8058E+00 0.3451E+00 0.1467E+00 0.6217E-01
0.2637E-01 0.1123E-01 0.4810E-02 0.2078E-02 0.9090E-03
0.4037E-03 0.1827E-03 0.8446E-04 0.4000E-04 0.1935E-04
0.9526E-05 0.4752E-05 0.2393E-05 0.1930E-05 0.1547E-05
0.1258E-05 0.1040E-05 0.8727E-06 0.7412E-06 0.6363E-06
0.5512E-06 0.4814E-06 0.4235E-06 0.3749E-06 0.3338E-06
0.2987E-06 0.2685E-06 0.2424E-06 0.1530E-06 0.1029E-06
0.7234E-07 0.5251E-07 0.3905E-07 0.2961E-07 0.2279E-07
0.1777E-07 0.1399E-07 0.1112E-07 0.8908E-08 0.7182E-08
0.5824E-08 0.4747E-08 0.3887E-08
END
N2O DENSITIES
0.7695E+13 0.6881E+13 0.6208E+13 0.5619E+13 0.5085E+13
0.4596E+13 0.4144E+13 0.3726E+13 0.3337E+13 0.2976E+13
0.2642E+13 0.2333E+13 0.2048E+13 0.1786E+13 0.1546E+13
0.1320E+13 0.1094E+13 0.9005E+12 0.7390E+12 0.6046E+12
0.4941E+12 0.4037E+12 0.3298E+12 0.2694E+12 0.2196E+12
0.1455E+12 0.9627E+11 0.6399E+11 0.3541E+11 0.1967E+11
0.9838E+10 0.4439E+10 0.2020E+10 0.1202E+10 0.7230E+09
0.4685E+09 0.3262E+09 0.2286E+09 0.1605E+09 0.1125E+09
0.7855E+08 0.5453E+08 0.3763E+08 0.2582E+08 0.1758E+08
0.1189E+08 0.7981E+07 0.5318E+07 0.3519E+07 0.2312E+07
0.1514E+07 0.9840E+06 0.6326E+06 0.4017E+06 0.2518E+06
0.1557E+06 0.9520E+05 0.5761E+05 0.3460E+05 0.2071E+05
0.1240E+05 0.7456E+04 0.4510E+04 0.2752E+04 0.1699E+04
0.1066E+04 0.6811E+03 0.4447E+03 0.2975E+03 0.2032E+03
0.1413E+03 0.9956E+02 0.7084E+02 0.5712E+02 0.4580E+02
0.3723E+02 0.3079E+02 0.2583E+02 0.2194E+02 0.1883E+02
0.1632E+02 0.1425E+02 0.1254E+02 0.1110E+02 0.9880E+01
0.8842E+01 0.7949E+01 0.7176E+01 0.4530E+01 0.3046E+01
0.2141E+01 0.1554E+01 0.1156E+01 0.8764E+00 0.6746E+00
0.5259E+00 0.4143E+00 0.3292E+00 0.2637E+00 0.2126E+00
0.1724E+00 0.1405E+00 0.1151E+00
END
NO2 DENSITIES
0.5589E+09 0.6058E+09 0.6575E+09 0.7142E+09 0.7757E+09
0.8413E+09 0.9104E+09 0.9822E+09 0.1056E+10 0.1131E+10
0.1205E+10 0.1277E+10 0.1345E+10 0.1408E+10 0.1463E+10
0.1509E+10 0.1548E+10 0.1578E+10 0.1603E+10 0.1626E+10
0.1698E+10 0.1723E+10 0.1921E+10 0.2041E+10 0.2351E+10
0.2526E+10 0.2518E+10 0.2522E+10 0.2128E+10 0.1804E+10
0.1411E+10 0.1022E+10 0.7460E+09 0.5193E+09 0.3657E+09

0.2485E+09 0.1627E+09 0.1071E+09 0.5419E+08 0.2738E+08
0.1378E+08 0.6901E+07 0.3435E+07 0.1699E+07 0.8343E+06
0.4068E+06 0.1970E+06 0.9465E+05 0.4513E+05 0.2137E+05
0.1009E+05 0.4727E+04 0.2191E+04 0.1004E+04 0.4536E+03
0.2023E+03 0.8918E+02 0.3891E+02 0.1686E+02 0.7284E+01
0.3150E+01 0.1368E+01 0.5978E+00 0.2645E+00 0.1185E+00
0.5421E-01 0.2541E-01 0.1217E-01 0.6160E-02 0.3184E-02
0.1460E-02 0.5917E-03 0.2421E-03 0.1953E-03 0.1565E-03
0.1273E-03 0.1052E-03 0.8830E-04 0.7500E-04 0.6438E-04
0.5577E-04 0.4871E-04 0.4285E-04 0.3793E-04 0.3377E-04
0.3022E-04 0.2717E-04 0.2453E-04 0.1548E-04 0.1041E-04
0.7319E-05 0.5313E-05 0.3951E-05 0.2996E-05 0.2306E-05
0.1798E-05 0.1416E-05 0.1125E-05 0.9013E-06 0.7266E-06
0.5892E-06 0.4803E-06 0.3933E-06
END
SO2 DENSITIES
0.7592E+10 0.6257E+10 0.4874E+10 0.3552E+10 0.2470E+10
0.1804E+10 0.1339E+10 0.1029E+10 0.8005E+09 0.6495E+09
0.5344E+09 0.4494E+09 0.3815E+09 0.3321E+09 0.2901E+09
0.2543E+09 0.2171E+09 0.1722E+09 0.1298E+09 0.9113E+08
0.6189E+08 0.4382E+08 0.3169E+08 0.2440E+08 0.1901E+08
0.1203E+08 0.7870E+07 0.5139E+07 0.3472E+07 0.2442E+07
0.1806E+07 0.1411E+07 0.1163E+07 0.1030E+07 0.9491E+06
0.9071E+06 0.8838E+06 0.8530E+06 0.7471E+06 0.6535E+06
0.5538E+06 0.4539E+06 0.3698E+06 0.2850E+06 0.2181E+06
0.1605E+06 0.1136E+06 0.7977E+05 0.5022E+05 0.3140E+05
0.1832E+05 0.9922E+04 0.5318E+04 0.2686E+04 0.1339E+04
0.6535E+03 0.3127E+03 0.1480E+03 0.6925E+02 0.3225E+02
0.1501E+02 0.6997E+01 0.3279E+01 0.1548E+01 0.7387E+00
0.3579E+00 0.1765E+00 0.8889E-01 0.4574E-01 0.2401E-01
0.1281E-01 0.6926E-02 0.3775E-02 0.2980E-02 0.2354E-02
0.1887E-02 0.1539E-02 0.1274E-02 0.1067E-02 0.9045E-03
0.7736E-03 0.6671E-03 0.5795E-03 0.5066E-03 0.4455E-03
0.3938E-03 0.3496E-03 0.3118E-03 0.1849E-03 0.1167E-03
0.7677E-04 0.5201E-04 0.3599E-04 0.2530E-04 0.1800E-04
0.1293E-04 0.9348E-05 0.6800E-05 0.4969E-05 0.3645E-05
0.2682E-05 0.1979E-05 0.1463E-05
END
NH3 DENSITIES
0.1265E+11 0.1142E+11 0.9562E+10 0.7103E+10 0.4872E+10
0.3119E+10 0.2013E+10 0.1225E+10 0.7194E+09 0.3733E+09
0.1784E+09 0.8460E+08 0.4292E+08 0.1854E+08 0.5710E+07
0.1977E+07 0.7967E+06 0.3528E+06 0.1819E+06 0.9113E+05
0.4675E+05 0.3151E+05 0.2391E+05 0.1874E+05 0.1441E+05
0.7980E+04 0.4555E+04 0.2435E+04 0.1154E+04 0.4994E+03
0.2126E+03 0.8386E+02 0.2514E+02 0.7212E+01 0.2279E+01
0.8269E+00 0.3498E+00 0.1708E+00 0.1154E+00 0.7783E-01
0.5360E-01 0.3764E-01 0.2628E-01 0.1876E-01 0.1330E-01
0.9447E-02 0.6720E-02 0.4746E-02 0.3367E-02 0.2373E-02
0.1673E-02 0.1174E-02 0.8156E-03 0.5615E-03 0.3815E-03
0.2567E-03 0.1713E-03 0.1130E-03 0.7408E-04 0.4835E-04
0.3154E-04 0.2062E-04 0.1355E-04 0.9033E-05 0.6087E-05
0.4158E-05 0.2888E-05 0.2048E-05 0.1488E-05 0.1103E-05
0.8317E-06 0.6356E-06 0.4899E-06 0.3867E-06 0.3055E-06
0.2448E-06 0.1997E-06 0.1653E-06 0.1385E-06 0.1174E-06
0.1004E-06 0.8657E-07 0.7520E-07 0.6574E-07 0.5781E-07

0.5110E-07 0.4537E-07 0.4046E-07 0.2400E-07 0.1514E-07
0.9963E-08 0.6749E-08 0.4670E-08 0.3283E-08 0.2336E-08
0.1677E-08 0.1213E-08 0.8824E-09 0.6449E-09 0.4730E-09
0.3480E-09 0.2568E-09 0.1898E-09
END